

Generalized local projection stabilized nonconforming finite element methods for Darcy equations

Deepika Garg · Sashikumaar Ganesan

Received date / Revised version date

Abstract An *a priori* analysis for a generalized local projection stabilized finite element solution of the Darcy equations is presented in this paper. A first-order nonconforming \mathbb{P}_1^{nc} finite element space is used to approximate the velocity, whereas the pressure is approximated using two different finite elements, namely piecewise constant \mathbb{P}_0 and piecewise linear nonconforming \mathbb{P}_1^{nc} elements. The considered finite element pairs, $\mathbb{P}_1^{nc}/\mathbb{P}_0$ and $\mathbb{P}_1^{nc}/\mathbb{P}_1^{nc}$, are inconsistent and incompatibility, respectively, for the Darcy problem. The stabilized discrete bilinear form satisfies an inf-sup condition with a generalized local projection norm. Moreover, *a priori* error estimates are established for both finite element pairs. Finally, the validation of the proposed stabilization scheme is demonstrated with appropriate numerical examples.

Keywords Finite element method · Darcy flows · Generalized local projection stabilization · Stability · Inf-sup condition · Nonconforming FEM · Error estimates

Mathematics Subject Classification (2010) 65N30 · 65N15 · 65N12 · 76M10

1 Introduction

The Darcy equations have considerable practical importance in the civil, geotechnical, petroleum, and electrical engineering fields such as flow in porous media, heat transfer, and semiconductor devices. In general, numerical schemes for the Darcy equations can be classified into two categories: (i) primal, the single-field formulation for the pressure, and (ii) mixed two-field formulation, where the pressure and velocity are approximated monolithically.

Deepika Garg

National Mathematics Initiative, Indian Institute of Science, Bengaluru 560012, India

E-mail: deepikagarg@iisc.ac.in, deepika.lpu.pbi@gmail.com

Sashikumaar Ganesan

Department of Computational and Data Sciences, Indian Institute of Science, Bengaluru 560012, India

E-mail: sashi@iisc.ac.in

The mixed two-field formulation eliminates the velocity, and it results in scalar second-order elliptic partial differential equations (PDEs) for the pressure. This pressure Poisson problem can be solved with adequate accuracy using the existing finite element methods (FEMs). However, the velocity will be a derived flux, and thus, its accuracy will be one order less than the accuracy of the pressure. Therefore, the second-order problem is preferred when pressure is the most significant variable, whereas the first-order system is preferred when velocity is more crucial [5, 37].

The mixed finite element method is a popular approach for solving PDEs with coupled unknown functions. The classical mixed variational formulation of the Darcy equations is posed in the function spaces $H(\text{div}, \Omega)$ and $L_0^2(\Omega)$ for the velocity and pressure respectively. Here, $H(\text{div}, \Omega)$ is the space of Lebesgue square-integrable functions, whose divergence is also Lebesgue square-integrable; $L_0^2(\Omega)$ is the space of Lebesgue square-integrable functions defined on Ω , modulo a constant. The finite dimensional subspaces of $H(\text{div}, \Omega)$ and $L_0^2(\Omega)$ are referred to as conforming approximation spaces. Moreover, this pair of approximation spaces has to satisfy the Babuška–Brezzi condition to obtain a stable approximation, mainly to avoid oscillations in the pressure approximation. Nevertheless, it is challenging to construct such finite element pairs that satisfy the inf-sup condition [25, pp. 85]. A well-known approach is the dual mixed formulation developed by RT (Raviart and Thomas [39]) and BDM (Brezzi, Douglas and Marini [12]) families, which requires the continuity of normal component of velocity in combination with a discontinuous pressure approximation. The mixed formulation has been used for various problems, see [3, 11–13, 18, 19, 23, 24, 26, 27]. A great accuracy has been achieved for both the velocity and the pressure. Further, the mass has been conserved very well locally and as well as globally. However, this approach has an inherent complexity; mainly, different interpolation spaces are required for pressure and velocity. It is more complex to implement, and it results in a saddle point system that is more challenging to solve.

In this study, we propose a mixed finite element formulation with a generalized local projection stabilized nonconforming finite element [20] method for the Darcy equations, which avoids the $H(\text{div}, \Omega)$ formulation. This approach significantly simplifies the problem.

It is well-known that the application of the standard Galerkin finite element method to the Darcy equations induces spurious oscillations in the numerical solution. Nevertheless, the standard Galerkin solution's stability and accuracy can be enhanced by applying a stabilization technique. The key idea in stabilization is to stabilize the Galerkin variational formulation by adding an artificial diffusion so that the discrete approximations are stable and convergent. The literature on stabilized FEM has become rich [5, 6, 14–17, 37, 40]. In this work, we concentrate on stabilization by local projections. The local projection stabilization (LPS) method has been proposed in [2, 9] for the Stokes problem and subsequently extended to various other classes of problems [8, 28, 29, 31, 35, 38, 42]. LPS is very attractive, particularly due to its commutation property in problems of optimization [7] and stabilization properties similar to those of residual-based approaches [34]. The local projection method's primary advantage is that the LPS approach adds symmetric and fewer stabilization terms than residual-based stabilization approaches. The generalized local projection stabilization (GLPS) is an extension of LPS to define local projection spaces on overlapping mesh cells. GLPS has first been introduced and studied for the convection–diffusion problem in [22, 33], for the Oseen problem in [4, 35] and recently, for the advection–reaction equations in [30]. GLPS is less sensitive to the

stabilization parameter [33], and thus, it reduces the ambiguity in using an optimal stabilization parameter, which is very challenging to identify for practical applications [32, 41]. Further, unlike LPS, GLPS needs neither a macro grid nor an enrichment of approximation spaces.

This paper's main contributions are developing a GLPS nonconforming finite element scheme for the Darcy equations and the derivation of its stability and convergence estimates. The number of degrees of freedom in nonconforming approximations will slightly be more than the conforming approximations. Nevertheless, the nonconforming method results in a system matrix with a smaller stencil. Moreover, system matrices with smaller stencils need less communication and facilitate scalable parallel numerical schemes. In the present analysis, two variants of approximations are considered for the Darcy equations. In the first variant, a piecewise linear nonconforming finite element for the velocity and a piecewise constant element for the pressure, i.e., $(\mathbb{P}_1^{nc}/\mathbb{P}_0)$ are used. The Crouzeix–Raviart space and piecewise constant polynomial space $(\mathbb{P}_1^{nc}/\mathbb{P}_0)$ are an inf-sup stable pair. However, it has been shown in [36] that the finite element pair $\mathbb{P}_1^{nc}/\mathbb{P}_0$ does not converge when applied to the Darcy problem. In this paper, this convergence issue is managed by GLPS. In the second variant, the pressure is also approximated using the linear nonconforming finite element, that is, \mathbb{P}_1^{nc} is used for both velocity and pressure. This equal order finite element pair does not satisfy the inf-sup compatibility, and the GLPS handles the inf-sup violation. Moreover, a convergence order of one is observed for the piecewise constant approximation of pressure with respect to a norm defined in (3.16), and 1.5 is observed for the \mathbb{P}_1^{nc} finite element approximation of pressure in a norm defined in (4.40).

The article's outline is as follows: in Section 2, the Darcy equations' variational formulation is introduced. Section 3 is devoted to a generalized local projection stabilization finite element method with a piecewise constant approximation of the pressure. Further, the stability results and *a priori* error estimates are derived for a proposed stabilized method. In Section 4, the stability and error analysis for the piecewise linear approximation for pressure are presented. In Section 5, numerical experiments are performed to validate the derived theoretical estimates. Section 6 provides a summary of the study.

2 Model problem

Consider the governing equations of a Darcy flow: Find (\mathbf{u}, p) such that

$$\begin{aligned} \mathbf{u} + \omega \nabla p &= \mathbf{f}; \quad \nabla \cdot \mathbf{u} = \phi \quad \text{in } \Omega, \\ \mathbf{u} \cdot \mathbf{n} &= \psi \quad \text{on } \partial\Omega, \end{aligned} \quad (2.1)$$

where $\Omega \subset \mathbb{R}^2$ is a bounded polygonal domain with boundary $\partial\Omega$. Here, \mathbf{u} is the velocity of the fluid, p is the pressure in the fluid, $\mathbf{f} \in [L^2(\Omega)]^2$ is the source function, ϕ is the volumetric flow rate source, $\psi \in H^{1/2}(\partial\Omega)$ is a given prescribed flux at the boundary, $\omega = \kappa/\lambda$, $\kappa > 0$ is the permeability and $\lambda > 0$ is the viscosity. The divergence constraint imposes that the prescribed data must satisfy

$$\int_{\Omega} \phi \, dx = \int_{\partial\Omega} \psi \, ds.$$

2.1 Variational formulation

Consider the Sobolev spaces:

$$\mathbf{V} := \{\mathbf{v} \in \mathbf{H}(\operatorname{div}, \Omega) \mid \mathbf{v} \cdot \mathbf{n} = 0 \text{ on } \partial\Omega\},$$

$$Q := L_0^2(\Omega) = \left\{ q \in L^2(\Omega) \mid \int_{\Omega} q dx = 0 \right\},$$

where $L^2(\Omega)$ is the space of square-integrable functions. Moreover, $L^2(\Omega)$ and $L_{\infty}(\Omega)$ norms are respectively denoted by $\|u\|$ and $\|u\|_{\infty}$. The standard notation of Sobolev space $\mathbf{H}^m(\Omega)$ for $m=1,2$ and its norm $\|\cdot\|_m$ are used. The notations $[L^2(\Omega)]^2$ and $[\mathbf{H}^1(\Omega)]^2$ respectively abbreviate the vector-valued versions of $L^2(\Omega)$ and $\mathbf{H}^1(\Omega)$; $\mathbf{H}_0^1(\Omega)$ is a subspace of $\mathbf{H}^1(\Omega)$ with zero trace functions. Multiplying the model equation (2.1) by test functions, integrate it over Ω and applying the integration by part to the pressure term results in a variational form:

Find $(\mathbf{u}, p) \in \mathbf{V} \times Q$ such that

$$a(\mathbf{u}, \mathbf{v}) - b(p, \mathbf{v}) = (\mathbf{f}, \mathbf{v}); \quad b(\mathbf{u}, q) = (\phi, q),$$

for all $(\mathbf{v}, q) \in \mathbf{V} \times Q$. Here,

$$a(\mathbf{u}, \mathbf{v}) := \int_{\Omega} \omega^{-1}(\mathbf{u} \cdot \mathbf{v}) dx; \quad b(p, \mathbf{v}) := (p, \nabla \cdot \mathbf{v}),$$

where (\cdot, \cdot) is the $L^2(\Omega)$ inner product. Further, the variational form can be written in a compact form: Find $(\mathbf{u}, p) \in \mathbf{V} \times Q$ such that

$$A((\mathbf{u}, p), (\mathbf{v}, q)) = l(\mathbf{v}) \tag{2.2}$$

for all $(\mathbf{v}, q) \in \mathbf{V} \times Q$, where

$$A((\mathbf{u}, p), (\mathbf{v}, q)) := a(\mathbf{u}, \mathbf{v}) - b(p, \mathbf{v}) + b(q, \mathbf{u}),$$

$$l(\mathbf{v}) := (\mathbf{f}, \mathbf{v}) + (\phi, q).$$

The well-posedness of the model problem (2.1) is an application of the Lax–Milgram lemma [25] and the Babuška–Brezzi condition for the pair $\mathbf{V} \times Q$ [25].

2.2 Finite element formulation

Let \mathcal{T}_h be a collection of non-overlapping quasi-uniform triangles obtained by decomposition of Ω . Let $h_K = \operatorname{diam}(K)$ for all $K \in \mathcal{T}_h$ and the mesh-size $h = \max_{K \in \mathcal{T}_h} h_K$. Let $\mathcal{E}_h = \mathcal{E}_h^I \cup \mathcal{E}_h^B$ be the set of all edges in \mathcal{T}_h , where \mathcal{E}_h^I and \mathcal{E}_h^B are the sets of all interior and boundary edges respectively and $h_E = \operatorname{diam}(E)$ for all $E \in \mathcal{E}_h$. Further, for each edge E in \mathcal{E}_h , a unit normal vector \mathbf{n} is associated; this is taken to be the unit outward normal to $\partial\Omega$ for all $E \in \mathcal{E}_h^B$. Suppose $K^+(E)$ and $K^-(E)$ are the neighbours of the interior edge $E \in \mathcal{E}_h^I$, then the normal vector \mathbf{n} is oriented from $K^+(E)$ and $K^-(E)$, see Figure 1. Similarly, for $v \in L^2(\Omega)$, the trace of v along one side of a cell is well-defined whereas

there are two traces for the edges sharing two cells. In such cases, the average and jump of a function v on the edge E can be defined as

$$\{v\} = \frac{1}{2}(v^+|_E + v^-|_E), \quad [v] := v^+|_E - v^-|_E,$$

where $v^\pm := v|_{K^\pm}$. Further, the average and jump of the vector-valued function \mathbf{v} are defined component-wise. Moreover, for any $E \in \mathcal{E}_h$, \mathcal{M}_E (patch of E) denotes the union of all cells that share the edge E , see Figure 1. The following norm is used in the analysis. Let the piecewise constant function $h_{\mathcal{T}}$ be defined by $h_{\mathcal{T}}|_K = h_K$ and $s \in \mathbb{R}$ and $m \geq 0$. Then,

$$\|h_{\mathcal{T}}^s u\|_m = \left(\sum_{K \in \mathcal{T}_h} h_K^{2s} \|u\|_{\mathbf{H}^m(K)}^2 \right)^{\frac{1}{2}} \quad \text{for all } u \in \mathbf{H}^m(\mathcal{T}_h).$$

For any $E \in \mathcal{E}_h$, define the fluctuation operator $\kappa_E: \mathbf{L}^2(\mathcal{M}_E) \rightarrow \mathbf{L}^2(\mathcal{M}_E)$ by

$$\kappa_E(v) := v - \frac{1}{|\mathcal{M}_E|} \int_{\mathcal{M}_E} v \, dx,$$

where $|\mathcal{M}_E|$ denotes the area of \mathcal{M}_E . Then,

$$\|\kappa_E\|_{\mathcal{L}(\mathbf{L}^2(\mathcal{M}_E), \mathbf{L}^2(\mathcal{M}_E))} \leq C \quad \forall E \in \mathcal{E}_h,$$

where C is a constant independent of h . Let $k \geq 0$ be an integer. Define the piecewise polynomial

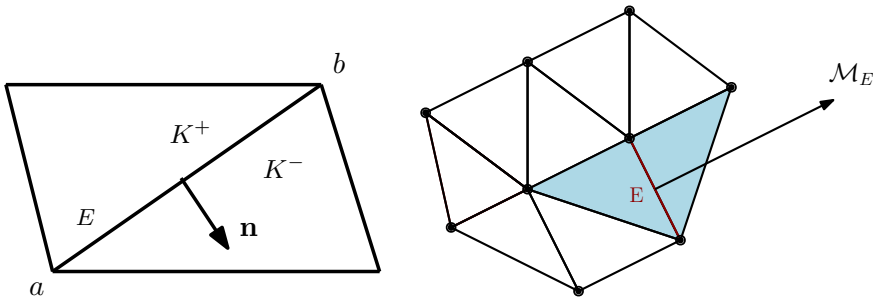


Fig. 1 Left side two neighbouring triangles K^+ and K^- are shared by the edge $E=ab$ with the initial node a and the end node b and \mathbf{n} is the unit outward normal to K^+ ; right side edge patch \mathcal{M}_E .

space as

$$\mathbb{P}_k(\mathcal{T}_h) := \{v \in \mathbf{L}^2(\Omega) : v|_K \in \mathbb{P}_k(K) \quad \text{for all } K \in \mathcal{T}_h\},$$

where $\mathbb{P}_k(K)$ is the space of polynomials of degree at most k over the element K . Further, define the piecewise linear nonconforming Crouzeix–Raviart finite element space as

$$\mathbb{P}_1^{nc}(\mathcal{T}_h) := \left\{ v \in \mathbf{L}^2(\Omega) : v|_K \in \mathbb{P}_1(K) \quad \int_E [v] \, ds = 0, \quad \text{for all } E \in \mathcal{E}_h \right\}.$$

In addition, define

$$\mathbb{P}_{1,0}^{nc}(\mathcal{T}_h) := \{v \in \mathbb{P}_1^{nc}(\mathcal{T}_h) \mid v(\text{mid}(E)) = 0 \text{ for all } E \in \mathcal{E}_h^B\}.$$

Note that throughout this paper, C (sometimes subscripted) denotes a generic positive constant that may depend on the shape-regularity of the triangulation but is independent of the mesh-size. Further, the notation $c \lesssim d$ represents the inequality $c \leq Cd$. Next, the following technical results of finite element analysis are recalled.

Lemma 1 Trace inequality [21, pp. 27]: Suppose E denotes an edge of $K \in \mathcal{T}_h$. For $v|_K \in H^1(K)$ and $v_h \in \mathbb{P}_k(\mathcal{T}_h)$, there holds

$$\|v\|_{L^2(E)} \leq C \left(h_K^{-1/2} \|v\|_{L^2(K)} + h_K^{1/2} \|\nabla v\|_{L^2(K)} \right), \quad (2.3)$$

$$\|v_h\|_{L^2(E)} \leq Ch_K^{-1/2} \|v_h\|_{L^2(K)}. \quad (2.4)$$

Lemma 2 Inverse inequality [21, pp. 26]: Let $v \in \mathbb{P}_k(\mathcal{T}_h)$ for all $k \geq 0$. Then,

$$\|\nabla v\|_{L^2(K)} \leq Ch_K^{-1} \|v\|_{L^2(K)}. \quad (2.5)$$

Lemma 3 Poincaré inequality [10, pp. 104]: For a bounded and connected polygonal domain Ω and for any $v \in H^1(\Omega)$,

$$\left\| v - \frac{1}{|\Omega|} \int_{\Omega} v dx \right\|_{L^2(\Omega)} \leq Ch_{\Omega} \|\nabla v\|_{L^2(\Omega)}, \quad (2.6)$$

where h_{Ω} and $|\Omega|$ denote the diameter and measure of domain Ω ; the constant C is independent of the mesh-size h_{Ω} .

Further, for a locally quasi-uniform and shape-regular triangulation, the L^2 -orthogonal projection $I_h: L^2(\Omega) \rightarrow \mathbb{P}_1^{nc}(\mathcal{T}_h)$ satisfies the following approximation properties [1, 22].

Lemma 4 L^2 -orthogonal projections: The L^2 -projection $I_h: L^2(\Omega) \rightarrow \mathbb{P}_1^{nc}(\mathcal{T}_h)$ satisfies

$$\|h_{\mathcal{T}}^{-1}(v - I_h v)\| + \|\nabla(v - I_h v)\| \leq C \|h_{\mathcal{T}} v\|_2, \text{ for all } v \in H^2(\Omega), \quad (2.7)$$

For vector-valued functions, $\mathbf{I}_h: [L^2(\Omega)]^2 \rightarrow [\mathbb{P}_1^{nc}(\mathcal{T}_h)]^2$ satisfies

$$\|h_{\mathcal{T}}^{-1}(\mathbf{v} - \mathbf{I}_h \mathbf{v})\| + \|\nabla(\mathbf{v} - \mathbf{I}_h \mathbf{v})\| \leq C \|h_{\mathcal{T}} \mathbf{v}\|_2 \text{ for all } \mathbf{v} \in [H^2(\Omega)]^2. \quad (2.8)$$

Moreover, the trace inequality (2.3) over each edge implies

$$\left(\sum_{E \in \mathcal{E}_h} \|\mathbf{v} - \mathbf{I}_h \mathbf{v}\|_{L^2(E)}^2 \right)^{1/2} \leq C \|h_{\mathcal{T}}^{3/2} \mathbf{v}\|_2 \text{ for all } \mathbf{v} \in [H^2(\Omega)]^2. \quad (2.9)$$

The orthogonality relation for all $\mathbf{v}_h \in \mathbf{V}_h$ implies

$$(\mathbf{v} - \mathbf{I}_h \mathbf{v}, \mathbf{v}_h) = 0. \quad (2.10)$$

The following approximation estimates hold for the L^2 -orthogonal projection operator:

$$\|\mathbf{I}_h \mathbf{v}\| \leq \|\mathbf{v}\|, \quad \|h_{\mathcal{T}}^{-1} \mathbf{I}_h \mathbf{v}\| \leq C \|h_{\mathcal{T}}^{-1} \mathbf{v}\| \quad \text{and} \quad \|\nabla_h(\mathbf{I}_h \mathbf{v})\| \leq C \|\nabla_h \mathbf{v}\|. \quad (2.11)$$

The L^2 -projection, $\pi_h: L^2(\Omega) \rightarrow \mathbb{P}_0(\mathcal{T}_h)$ such that $(q - \pi_h q, r_h) = 0$ for all $r_h \in \mathbb{P}_0(\mathcal{T}_h)$ [25], has the following approximation property:

$$\|q - \pi_h q\| \leq C \|h_{\mathcal{T}} q\|_1 \quad \text{for all } q \in H^1(\Omega). \quad (2.12)$$

3 Piecewise constant approximation of pressure ($[\mathbb{P}_1^{nc}(\mathcal{T}_h)]^2 / \mathbb{P}_0(\mathcal{T}_h)$)

This section describes a generalized local projection stabilized finite element method for the problem (2.1), where the velocity is approximated with nonconforming (\mathbb{P}_1^{nc}) finite elements and the pressure with piecewise constants. The finite element pair $[\mathbb{P}_1^{nc}(\mathcal{T}_h)]^2 / \mathbb{P}_0(\mathcal{T}_h)$ is an inf-sup stable pair. However, this pair results in inconsistent discretizations for the Darcy equations [36]. Therefore, the GLPS method is introduced here to handle the inconsistency issue.

Let $\mathbf{V}_h := [\mathbb{P}_1^{nc}(\mathcal{T}_h)]^2$ and $Q_h := L_0^2(\Omega) \cap \mathbb{P}_0(\mathcal{T}_h)$. For each $E \in \mathcal{E}_h$, let $\beta_E := \beta h_E$ for some stabilization parameter $\beta \geq 0$ and let $S_h(\cdot, \cdot)$ be a stabilization term given by

$$S_h(\mathbf{u}_h, \mathbf{v}) := \sum_{E \in \mathcal{E}_h} \omega^{-1} \beta_E \int_{\mathcal{M}_E} \kappa_E (\nabla_h \cdot \mathbf{u}_h) \kappa_E (\nabla_h \cdot \mathbf{v}) dx + \sum_{E \in \mathcal{E}_h} \int_E \frac{1}{h_E} [\mathbf{u}_h \cdot \mathbf{n}] [\mathbf{v} \cdot \mathbf{n}] ds. \quad (3.13)$$

The generalized local projection stabilized discrete form of (2.1) reads as:

Find $(\mathbf{u}_h, p_h) \in \mathbf{V}_h \times Q_h$ such that

$$A_h((\mathbf{u}_h, p_h), (\mathbf{v}, q)) = l(\mathbf{v}, q) \quad \text{for all } (\mathbf{v}, q) \in \mathbf{V}_h \times Q_h, \quad (3.14)$$

where

$$A_h((\mathbf{u}_h, p_h), (\mathbf{v}, q)) := a_h(\mathbf{u}_h, \mathbf{v}) - b_h(p_h, \mathbf{v}) + b_h(q, \mathbf{u}_h) + S_h((\mathbf{u}_h, \mathbf{v}), \quad (3.15)$$

and

$$\begin{aligned} a_h(\mathbf{u}_h, \mathbf{v}) &:= \sum_{K \in \mathcal{T}_h} \int_K \omega^{-1} (\mathbf{u}_h \cdot \mathbf{v}) dx, \quad b_h(q, \mathbf{u}_h) := (q, \nabla_h \cdot \mathbf{u}_h)_{L^2(\Omega)} - \sum_{E \in \mathcal{E}_h^B} \int_E (\mathbf{u}_h \cdot \mathbf{n}) q ds, \\ S_h(\mathbf{u}_h, \mathbf{v}) &:= S_I(\mathbf{u}_h, \mathbf{v}) + S_B(\mathbf{u}_h, \mathbf{v}), \\ S_I(\mathbf{u}_h, \mathbf{v}) &:= \sum_{E \in \mathcal{E}_h} \omega^{-1} \beta_E \int_{\mathcal{M}_E} \kappa_E (\nabla_h \cdot \mathbf{u}_h) \kappa_E (\nabla_h \cdot \mathbf{v}) dx, \quad S_B(\mathbf{u}_h, \mathbf{v}) := \sum_{E \in \mathcal{E}_h} \int_E \frac{1}{h_E} [\mathbf{u}_h \cdot \mathbf{n}] [\mathbf{v} \cdot \mathbf{n}] ds, \\ l(\mathbf{v}, q) &:= (\mathbf{f}, \mathbf{v}) + (\phi, q) + \sum_{E \in \mathcal{E}_h^B} \left(- \int_E \psi q ds + \int_E \frac{1}{h_E} \psi (\mathbf{v} \cdot \mathbf{n}) ds \right). \end{aligned}$$

In the stabilization term, the additional edge integrals of the jump of the normal component of the discrete velocity along edges are necessary to control the nonconformity (consistency error) arising from the pressure terms [4, 15].

Further, the generalized local projection norm for $\mathbf{V}_h \times Q_h$ is defined by

$$\|(\mathbf{u}_h, p_h)\|_{\text{GLP}}^2 := \left\| \omega^{-\frac{1}{2}} \mathbf{u}_h \right\|^2 + \left\| h^{\frac{1}{2}} (\nabla_h \cdot \mathbf{u}_h) \right\|^2 + \|p_h\|^2 + S_h(\mathbf{u}_h, \mathbf{u}_h). \quad (3.16)$$

3.1 Stability

The main result of this section is the following theorem, which ensures that the discrete bilinear form is well-posed [25].

Theorem 1 *Suppose $\beta_E = \beta h_E$ for some $\beta > 0$. Then, the discrete bilinear form (3.14) satisfies the following inf-sup condition for some positive constant γ , independent of h :*

$$\inf_{(\mathbf{u}_h, p_h) \in \mathbf{V}_h \times Q_h} \sup_{(\mathbf{v}_h, q_h) \in \mathbf{V}_h \times Q_h} \frac{A_h((\mathbf{u}_h, p_h), (\mathbf{v}_h, q_h))}{\|(\mathbf{u}_h, p_h)\|_{\text{GLP}} \|(\mathbf{v}_h, q_h)\|_{\text{GLP}}} \geq \gamma > 0.$$

Proof. In order to prove the stability result, it is enough to choose some $(\mathbf{v}_h, q_h) \in \mathbf{V}_h \times Q_h$ for any arbitrary $(\mathbf{u}_h, p_h) \in \mathbf{V}_h \times Q_h$, such that

$$\frac{A_h((\mathbf{u}_h, p_h), (\mathbf{v}_h, q_h))}{\|(\mathbf{v}_h, q_h)\|_{\text{GLP}}} \geq \gamma \|(\mathbf{u}_h, p_h)\|_{\text{GLP}} > 0. \quad (3.17)$$

First, consider the bilinear form $A_h(\cdot, \cdot)$ defined in (3.15) with the test function pair $(\mathbf{v}_h, q_h) = (\mathbf{u}_h, p_h)$:

$$A_h((\mathbf{u}_h, p_h), (\mathbf{u}_h, p_h)) = \left\| \omega^{-\frac{1}{2}} \mathbf{u}_h \right\|^2 + S_h(\mathbf{u}_h, \mathbf{u}_h). \quad (3.18)$$

Since the pair $[\mathbb{P}_{1,0}^{\text{nc}}(\mathcal{T}_h)]^2 \times Q_h$ satisfies an inf-sup condition [25], i.e., there exists a constant $\mu > 0$ such that

$$\inf_{p_h \in Q_h} \sup_{\mathbf{v}_h \in [\mathbb{P}_{1,0}^{\text{nc}}(\mathcal{T}_h)]^2} \frac{(\text{div}_h \mathbf{v}_h, p_h)}{\|\nabla_h \mathbf{v}_h\| \|p_h\|} \geq \mu > 0. \quad (3.19)$$

As a consequence of (3.19), for each $p_h \in Q_h$, there exists $\mathbf{z}_h \in [\mathbb{P}_{1,0}^{\text{nc}}(\mathcal{T}_h)]^2$ such that

$$-(\text{div}_h \mathbf{z}_h, p_h) = \|p_h\|^2 \text{ and } \|\mathbf{z}_h\|_{1,h} \leq C_1 \|p_h\|, \quad (3.20)$$

where, the norm of \mathbf{z}_h is defined as $\|\mathbf{z}_h\|_{1,h} = \left(\sum_{K \in \mathcal{T}_h} \|\mathbf{z}_h\|_{1,K}^2 \right)^{1/2}$, [25]. Taking $(\mathbf{v}_h, q_h) = (\mathbf{z}_h, 0)$ as a test function pair, the bilinear form (3.15) becomes

$$A_h((\mathbf{u}_h, p_h), (\mathbf{z}_h, 0)) = a_h(\mathbf{u}_h, \mathbf{z}_h) - b_h(p_h, \mathbf{z}_h) + S_h(\mathbf{u}_h, \mathbf{z}_h). \quad (3.21)$$

Now, estimate the three terms of (3.21) individually. The first term is handled by using the Cauchy–Schwarz inequality, (3.20) and Young’s inequality, as

$$a_h(\mathbf{u}_h, \mathbf{z}_h) \leq \omega^{-1} \|\mathbf{u}_h\| \|\mathbf{z}_h\| \leq \omega^{-1} C_1 \|\mathbf{u}_h\| \|p_h\| \leq C \left\| \omega^{-\frac{1}{2}} \mathbf{u}_h \right\|^2 + \frac{1}{6} \|p_h\|^2. \quad (3.22)$$

The constant C in (3.22) depend on ω^{-1} . Using (3.20) in the second term of (3.21),

$$-b_h(p_h, \mathbf{z}_h) = -(p_h, \nabla_h \cdot \mathbf{z}_h) + \sum_{E \in \mathcal{E}_h^B} \int_E (\mathbf{z}_h \cdot \mathbf{n}) p_h ds = \|p_h\|^2 + \sum_{E \in \mathcal{E}_h^B} \int_E (\mathbf{z}_h \cdot \mathbf{n}) p_h ds.$$

For any $E \in \mathcal{E}_h^B$, the edge integral of \mathbf{z}_h vanishes as $\mathbf{z}_h \in [\mathbb{P}_{1,0}^{nc}(\mathcal{T}_h)]^2$. Since p_h are constants on the edges,

$$\sum_{E \in \mathcal{E}_h^B} \int_E (\mathbf{z}_h \cdot \mathbf{n}) p_h ds = 0 \text{ for all } E \in \mathcal{E}_h^B.$$

Recall the stabilization term

$$S_h(\mathbf{u}_h, \mathbf{z}_h) = \sum_{E \in \mathcal{E}_h} \omega^{-1} \beta_E (\kappa_E(\nabla_h \cdot \mathbf{u}_h), \kappa_E(\nabla_h \cdot \mathbf{z}_h))_{L^2(\mathcal{M}_E)} + \sum_{E \in \mathcal{E}_h} \int_E \frac{1}{h_E} [\mathbf{u}_h \cdot \mathbf{n}] [\mathbf{z}_h \cdot \mathbf{n}] ds. \quad (3.23)$$

Applying the Cauchy–Schwarz inequality, boundedness of the patch-wise local projection operator, (3.20) and Young’s inequality in the first term of (3.23),

$$\begin{aligned} & \sum_{E \in \mathcal{E}_h} \omega^{-1} \beta_E (\kappa_E(\nabla_h \cdot \mathbf{u}_h), \kappa_E(\nabla_h \cdot \mathbf{z}_h))_{L^2(\mathcal{M}_E)} \\ & \leq \left(\sum_{E \in \mathcal{E}_h} \omega^{-1} \beta_E \|\kappa_E(\nabla_h \cdot \mathbf{u}_h)\|_{L^2(\mathcal{M}_E)}^2 \right)^{\frac{1}{2}} \left(\sum_{E \in \mathcal{E}_h} \omega^{-1} \beta_E \|\kappa_E(\nabla_h \cdot \mathbf{z}_h)\|_{L^2(\mathcal{M}_E)}^2 \right)^{\frac{1}{2}} \\ & = \left(\sum_{E \in \mathcal{E}_h} \omega^{-1} \beta_E \|\kappa_E(\nabla_h \cdot \mathbf{u}_h)\|_{L^2(\mathcal{M}_E)}^2 \right)^{\frac{1}{2}} \left(\sum_{E \in \mathcal{E}_h} \omega^{-1} \beta_E \left\| \nabla_h \cdot \mathbf{z}_h - \frac{1}{|\mathcal{M}_E|} \int_{\mathcal{M}_E} \nabla_h \cdot \mathbf{z}_h dx \right\|_{L^2(\mathcal{M}_E)}^2 \right)^{\frac{1}{2}} \\ & \leq C_1 [S_h(\mathbf{u}_h, \mathbf{u}_h)]^{\frac{1}{2}} \|\nabla_h \cdot \mathbf{z}_h\| \\ & \leq \frac{C}{4} S_h(\mathbf{u}_h, \mathbf{u}_h) + \frac{1}{6} \|p_h\|. \end{aligned}$$

The constant C in the above estimates depend on $\omega^{-1/2}$. Using the continuity of nonconforming finite element functions at all the mid points of the inner edges, $\int_E [u_h] ds = 0$ for all $u_h \in \mathbb{P}_1^{nc}(\mathcal{T}_h)$ and $E \in \mathcal{E}_h^I$. Applying the Poincaré inequality and trace inequality for $\mathbf{z}_h \in [\mathbb{P}_{1,0}^{nc}(\mathcal{T}_h)]^2$ and $E \in \mathcal{E}_h^I$,

$$\|\mathbf{z}_h\|_{L^2(E)} \leq Ch_E^{\frac{1}{2}} \|\nabla_h \mathbf{z}_h\|_{L^2(\mathcal{M}_E)}.$$

An addition over all the edges and using the the Cauchy–Schwarz inequality and (3.20),

$$\begin{aligned} \sum_{E \in \mathcal{E}_h} \int_E \frac{1}{h_E} [\mathbf{u}_h \cdot \mathbf{n}] [\mathbf{z}_h \cdot \mathbf{n}] ds &\leq \left(\sum_{E \in \mathcal{E}_h} \int_E \frac{1}{h_E} [\mathbf{u}_h \cdot \mathbf{n}]^2 ds \right)^{\frac{1}{2}} \left(\sum_{E \in \mathcal{E}_h} \int_E \frac{1}{h_E} [\mathbf{z}_h \cdot \mathbf{n}]^2 ds \right)^{\frac{1}{2}} \\ &\leq \frac{C}{4} \sum_{E \in \mathcal{E}_h} \int_E \frac{1}{h_E} [\mathbf{u}_h \cdot \mathbf{n}]^2 ds + \frac{\|p_h\|^2}{6}. \end{aligned}$$

Thus,

$$S_h(\mathbf{u}_h, \mathbf{z}_h) \leq \frac{C}{2} S_h(\mathbf{u}_h, \mathbf{u}_h) + \frac{1}{3} \|p_h\|^2.$$

Put together, (3.21) leads to

$$A_h((\mathbf{u}_h, p_h), (\mathbf{z}_h, 0)) \geq \frac{1}{2} \|p_h\|^2 - C \left(\|\omega^{-\frac{1}{2}} \mathbf{u}_h\|^2 + \frac{1}{2} S_h(\mathbf{u}_h, \mathbf{u}_h) \right). \quad (3.24)$$

Further, the control of $\left\| h_{\mathcal{T}}^{\frac{1}{2}} (\nabla_h \cdot \mathbf{u}_h) \right\|^2$ can be obtained by choosing $(\mathbf{v}_h, q_h) = (0, h_{\mathcal{T}} (\nabla_h \cdot \mathbf{u}_h))$ in (3.15), that is,

$$A_h((\mathbf{u}_h, p_h), (0, h_{\mathcal{T}} (\nabla_h \cdot \mathbf{u}_h))) = b_h(h_{\mathcal{T}} (\nabla_h \cdot \mathbf{u}_h), \mathbf{u}_h). \quad (3.25)$$

Consider the right-hand side term of (3.25):

$$\begin{aligned} b_h(h_{\mathcal{T}} (\nabla_h \cdot \mathbf{u}_h), \mathbf{u}_h) &= (h_{\mathcal{T}} (\nabla_h \cdot \mathbf{u}_h), \nabla_h \cdot \mathbf{u}_h) - \sum_{E \in \mathcal{E}_h^B} \int_E (\mathbf{u}_h \cdot \mathbf{n}) h_E (\nabla_h \cdot \mathbf{u}_h) ds \\ &= \left\| h_{\mathcal{T}}^{\frac{1}{2}} (\nabla_h \cdot \mathbf{u}_h) \right\|^2 - \sum_{E \in \mathcal{E}_h^B} \int_E h_E (\mathbf{u}_h \cdot \mathbf{n}) (\nabla_h \cdot \mathbf{u}_h) ds. \end{aligned}$$

Using the Cauchy–Schwarz inequality,

$$\begin{aligned} \sum_{E \in \mathcal{E}_h^B} \int_E h_E (\mathbf{u}_h \cdot \mathbf{n}) (\nabla_h \cdot \mathbf{u}_h) ds &\leq \sum_{E \in \mathcal{E}_h^B} h_E \|\mathbf{u}_h \cdot \mathbf{n}\|_{L^2(E)} \|\nabla_h \cdot \mathbf{u}_h\|_{L^2(E)} \\ &\leq \left(\sum_{E \in \mathcal{E}_h^B} \frac{1}{h_E} \|\mathbf{u}_h \cdot \mathbf{n}\|_{L^2(E)}^2 \right)^{\frac{1}{2}} \left(\sum_{E \in \mathcal{E}_h^B} h_E^3 \|\nabla_h \cdot \mathbf{u}_h\|_{L^2(E)}^2 \right)^{\frac{1}{2}} \\ &\leq \left(\sum_{E \in \mathcal{E}_h^B} \int_E \frac{1}{h_E} (\mathbf{u}_h \cdot \mathbf{n})^2 ds \right)^{\frac{1}{2}} \left(\sum_{E \in \mathcal{E}_h^B} h_E^2 \left\| h_{\mathcal{T}}^{\frac{1}{2}} (\nabla_h \cdot \mathbf{u}_h) \right\|_{L^2(E)}^2 \right)^{\frac{1}{2}}. \end{aligned}$$

Applying the trace inequality (2.4),

$$\left\| h_{\mathcal{T}}^{\frac{1}{2}} (\nabla_h \cdot \mathbf{u}_h) \right\|_{L^2(E)} \leq h_K^{-1/2} \left\| h_{\mathcal{T}}^{\frac{1}{2}} (\nabla_h \cdot \mathbf{u}_h) \right\|_{L^2(K)},$$

$$\sum_{E \in \mathcal{E}_h^B} \int_E h_E (\mathbf{u}_h \cdot \mathbf{n}) (\nabla_h \cdot \mathbf{u}_h) ds \leq C \left\| h_{\mathcal{T}}^{\frac{1}{2}} (\nabla_h \cdot \mathbf{u}_h) \right\| \left[S_B(\mathbf{u}_h, \mathbf{u}_h) \right]^{\frac{1}{2}} \leq \frac{1}{2} \left\| h_{\mathcal{T}}^{\frac{1}{2}} (\nabla_h \cdot \mathbf{u}_h) \right\|^2 + \frac{C}{2} S_B(\mathbf{u}_h, \mathbf{u}_h).$$

Put together, (3.25) leads to

$$A_h((\mathbf{u}_h, p_h), (0, h_{\mathcal{T}}(\nabla_h \cdot \mathbf{u}_h))) \geq \frac{1}{2} \left\| h_{\mathcal{T}}^{\frac{1}{2}} (\nabla_h \cdot \mathbf{u}_h) \right\|^2 - \frac{C}{2} S_h(\mathbf{u}_h, \mathbf{u}_h). \quad (3.26)$$

The selection of (\mathbf{v}_h, q_h) is

$$(\mathbf{v}_h, q_h) = (\mathbf{u}_h, p_h) + \frac{1}{C+1} (\mathbf{z}_h, 0) + \frac{1}{C+1} (0, h_{\mathcal{T}}(\nabla_h \cdot \mathbf{u}_h)).$$

Adding (3.18), (3.24) and (3.26),

$$\begin{aligned} A_h((\mathbf{u}_h, p_h), (\mathbf{v}_h, q_h)) &\geq \left\| \omega^{-\frac{1}{2}} \mathbf{u}_h \right\|^2 + S_h(\mathbf{u}_h, \mathbf{u}_h) + \frac{1}{2+2C} \|p_h\|^2 - \frac{C}{C+1} \left(\left\| \omega^{-\frac{1}{2}} \mathbf{u}_h \right\|^2 + \frac{1}{2} S_h(\mathbf{u}_h, \mathbf{u}_h) \right) \\ &\quad + \frac{1}{2+2C} \left\| h_{\mathcal{T}}^{\frac{1}{2}} (\nabla_h \cdot \mathbf{u}_h) \right\|^2 - \frac{C}{2+2C} (S_h(\mathbf{u}_h, \mathbf{u}_h)) \\ &= \frac{1}{2+2C} \|p_h\|^2 + \frac{1}{2+2C} \left\| h_{\mathcal{T}}^{\frac{1}{2}} (\nabla_h \cdot \mathbf{u}_h) \right\|^2 + \left(1 - \frac{C}{1+C}\right) \left(\left\| \omega^{-\frac{1}{2}} \mathbf{u}_h \right\|^2 + S_h(\mathbf{u}_h, \mathbf{u}_h) \right) \\ &\geq \frac{1}{2+2C} \|p_h\|^2 + \frac{1}{2+2C} \left\| h_{\mathcal{T}}^{\frac{1}{2}} (\nabla_h \cdot \mathbf{u}_h) \right\|^2 + \frac{1}{C+1} \left(\left\| \omega^{-\frac{1}{2}} \mathbf{u}_h \right\|^2 + S_h(\mathbf{u}_h, \mathbf{u}_h) \right) \\ &\geq \frac{1}{2C+2} |||(\mathbf{u}_h, p_h)|||_{\text{GLP}}^2. \end{aligned} \quad (3.27)$$

The triangle inequality implies

$$\begin{aligned} |||(\mathbf{v}_h, q_h)|||_{\text{GLP}} &\leq |||(\mathbf{u}_h, p_h)|||_{\text{GLP}} + \frac{1}{C+1} |||(\mathbf{z}_h, 0)|||_{\text{GLP}} + \frac{1}{C+1} |||(0, h_{\mathcal{T}}(\nabla_h \cdot \mathbf{u}_h))|||_{\text{GLP}} \\ &\leq \alpha |||(\mathbf{u}_h, p_h)|||_{\text{GLP}}, \end{aligned} \quad (3.28)$$

where, in the second term on the right-hand side of (3.28), using (3.20) and boundedness of the patch-wise local projection operator,

$$|||(\mathbf{z}_h, 0)|||_{\text{GLP}} = \left\| \omega^{-\frac{1}{2}} \mathbf{z}_h \right\|^2 + \left\| h_{\mathcal{T}}^{\frac{1}{2}} (\nabla_h \cdot \mathbf{z}_h) \right\|^2 + S_h(\mathbf{z}_h, \mathbf{z}_h) \leq C \|p_h\|^2.$$

The constant C in the above estimates depend on ω^{-1} . Using an inverse inequality in the third term on the right-hand side of (3.28),

$$|||(0, h_{\mathcal{T}}(\nabla_h \cdot \mathbf{u}_h))|||_{\text{GLP}} = \|h_{\mathcal{T}}(\nabla_h \cdot \mathbf{u}_h)\|^2 \leq C \left\| \omega^{-\frac{1}{2}} \mathbf{u}_h \right\|^2.$$

The constant C in the above estimates depend on ω . Finally, (3.27) and (3.28) lead to (3.17) and conclude the proof.

3.2 *A priori* error estimates

This subsection discusses *a priori* error estimates for the $([\mathbb{P}_1^{nc}(\mathcal{T}_h)]^2/\mathbb{P}_0(\mathcal{T}_h))$ approximation for velocity–pressure pair with respect to the GLP norm.

Lemma 5 *Suppose $\beta_E = \beta h_E$ for some $\beta > 0$. For any $(\mathbf{u}, p) \in [\mathbf{H}^2(\Omega)]^2 \times \mathbf{L}_0^2 \cap \mathbf{H}^1(\Omega)$ it holds that*

$$\|(\mathbf{u} - \mathbf{I}_h \mathbf{u}, p - \pi_h p)\|_{\text{GLP}} \leq C \left(\|h_{\mathcal{T}} \mathbf{u}\|_2 + \|h_{\mathcal{T}} p\|_1 \right). \quad (3.29)$$

Proof. First, consider the terms in the GLP norm defined in (3.16):

$$\begin{aligned} \|(\mathbf{u} - \mathbf{I}_h \mathbf{u}, p - \pi_h p)\|_{\text{GLP}}^2 &:= \left\| \omega^{-\frac{1}{2}} (\mathbf{u} - \mathbf{I}_h \mathbf{u}) \right\|^2 + \|h_{\mathcal{T}}^{\frac{1}{2}} (\nabla_h \cdot (\mathbf{u} - \mathbf{I}_h \mathbf{u}))\|^2 + \|p - \pi_h p\|^2 \\ &\quad + S_h(\mathbf{u} - \mathbf{I}_h \mathbf{u}, \mathbf{u} - \mathbf{I}_h \mathbf{u}). \end{aligned}$$

Using the projection estimates (2.8) and (2.12),

$$\left\| \omega^{-\frac{1}{2}} (\mathbf{u} - \mathbf{I}_h \mathbf{u}) \right\| \leq C \|h_{\mathcal{T}}^2 \mathbf{u}\|_2, \quad \|h_{\mathcal{T}}^{\frac{1}{2}} (\nabla_h \cdot (\mathbf{u} - \mathbf{I}_h \mathbf{u}))\| \leq \left\| h_{\mathcal{T}}^{\frac{3}{2}} \mathbf{u} \right\|_2 \quad \text{and} \quad \|p - \pi_h p\| \leq \|h_{\mathcal{T}} p\|_1.$$

Note that the constant C in the above estimates depend on $\omega^{-1/2}$. Using the boundedness of the patch-wise local projection operator, $\beta_E = \beta h_E$ for some $\beta > 0$, and (2.8),

$$\begin{aligned} S_I(\mathbf{u} - \mathbf{I}_h \mathbf{u}, \mathbf{u} - \mathbf{I}_h \mathbf{u}) &= \sum_{E \in \mathcal{E}_h} \omega^{-1} \beta_E \int_{\mathcal{M}_E} \kappa_E^2 (\nabla_h \cdot (\mathbf{u} - \mathbf{I}_h \mathbf{u})) \, dx \\ &\leq C \sum_{E \in \mathcal{E}_h} \omega^{-1} \beta_E \|\nabla_h \cdot (\mathbf{u} - \mathbf{I}_h \mathbf{u})\|_{\mathbf{L}^2(\mathcal{M}_E)}^2 \leq C_1 \left\| h_{\mathcal{T}}^{3/2} \mathbf{u} \right\|_2^2. \end{aligned}$$

Note that the constant C_1 in the above estimates depend on ω^{-1} . At the edge E , the jump term has contribution for both cells sharing that edge. Using the trace inequality (2.3),

$$\|[\mathbf{u} - \mathbf{I}_h \mathbf{u}]\|_{\mathbf{L}^2(E)} \leq C \left(h_E^{-1/2} \|\mathbf{u} - \mathbf{I}_h \mathbf{u}\|_{\mathbf{L}^2(\mathcal{M}_E)} + h_E^{1/2} \|\nabla_h (\mathbf{u} - \mathbf{I}_h \mathbf{u})\|_{\mathbf{L}^2(\mathcal{M}_E)} \right),$$

and using the projection estimates (2.8)–(2.9),

$$S_B(\mathbf{u} - \mathbf{I}_h \mathbf{u}, \mathbf{u} - \mathbf{I}_h \mathbf{u}) = \sum_{E \in \mathcal{E}_h} \int_E \frac{1}{h_E} [(\mathbf{u} - \mathbf{I}_h \mathbf{u}) \cdot \mathbf{n}]^2 \, ds \leq \|h_{\mathcal{T}} \mathbf{u}\|_2^2.$$

The combination of the above estimates leads to (3.29). This concludes the proof.

Lemma 6 *Suppose $\beta_E = \beta h_E$ for some $\beta > 0$. Let $(\mathbf{u}, p) \in [\mathbf{H}^2(\Omega)]^2 \times \mathbf{L}_0^2 \cap \mathbf{H}^1(\Omega)$ and for all $(\mathbf{v}_h, q_h) \in \mathbf{V}_h \times \mathbf{Q}_h$. Then,*

$$A_h((\mathbf{u} - \mathbf{I}_h \mathbf{u}, p - \pi_h p), (\mathbf{v}_h, q_h)) \leq C \left(\|h_{\mathcal{T}} \mathbf{u}\|_2 + \|h_{\mathcal{T}} p\|_1 \right) \|(\mathbf{v}_h, q_h)\|_{\text{GLP}}. \quad (3.30)$$

Proof. Consider the bilinear form in (3.15):

$$A_h((\mathbf{u} - \mathbf{I}_h \mathbf{u}, p - \pi_h p), (\mathbf{v}_h, q_h)) = a_h(\mathbf{u} - \mathbf{I}_h \mathbf{u}, \mathbf{v}_h) - b_h(p - \pi_h p, \mathbf{v}_h) + b_h(q_h, \mathbf{u} - \mathbf{I}_h \mathbf{u}) + S_h(\mathbf{u} - \mathbf{I}_h \mathbf{u}, \mathbf{v}_h). \quad (3.31)$$

The first term is handled by using the Cauchy–Schwarz inequality and projection estimates (2.8), as

$$a_h(\mathbf{u}-\mathbf{I}_h\mathbf{u},\mathbf{v}_h)\leq\left\|\omega^{-\frac{1}{2}}(\mathbf{u}-\mathbf{I}_h\mathbf{u})\right\|\left\|\omega^{-\frac{1}{2}}\mathbf{v}_h\right\|\leq C\|h_{\mathcal{T}}^2\mathbf{u}\|_2\|(\mathbf{v}_h,q_h)\|_{\text{GLP}}.$$

Note that the constant C in the above estimates depend on $\omega^{-1/2}$. Consider the second term on the right-hand side of (3.31):

$$b_h(p-\pi_h p,\mathbf{v}_h)=(p-\pi_h p,\nabla_h\cdot\mathbf{v}_h)-\sum_{E\in\mathcal{E}_h^B}\int_E(\mathbf{v}_h\cdot\mathbf{n})(p-\pi_h p)ds. \quad (3.32)$$

Applying the L^2 -orthogonal projection property (2.12), the first term on the right-hand side of (3.32) gives $(p-\pi_h p,\nabla_h\cdot\mathbf{v}_h)=0$. The second term is handled by using the Cauchy–Schwarz inequality, trace inequality over the edges and (2.12), as

$$\begin{aligned} \sum_{E\in\mathcal{E}_h^B}\int_E(\mathbf{v}_h\cdot\mathbf{n})(p-\pi_h p)ds &\leq\left(\sum_{E\in\mathcal{E}_h^B}\int_E\frac{1}{h_E}(\mathbf{v}_h\cdot\mathbf{n})^2ds\right)^{\frac{1}{2}}\left(\sum_{E\in\mathcal{E}_h^B}h_E\|p-\pi_h p\|_{L^2(E)}^2\right)^{\frac{1}{2}} \\ &\leq\|h_{\mathcal{T}}p\|_1\|(\mathbf{v}_h,q_h)\|_{\text{GLP}}. \end{aligned}$$

Consider the next term on the right-hand side of (3.31):

$$b_h(q_h,\mathbf{u}-\mathbf{I}_h\mathbf{u})=(q_h,\nabla_h\cdot(\mathbf{u}-\mathbf{I}_h\mathbf{u}))- \sum_{E\in\mathcal{E}_h^B}\int_E((\mathbf{u}-\mathbf{I}_h\mathbf{u})\cdot\mathbf{n})q_hds. \quad (3.33)$$

Applying the Cauchy–Schwarz inequality and projection estimates (2.8), the first term of (3.33) is estimated as:

$$(q_h,\nabla_h\cdot(\mathbf{u}-\mathbf{I}_h\mathbf{u}))\leq\|q_h\|\|\nabla_h\cdot(\mathbf{u}-\mathbf{I}_h\mathbf{u})\|\leq C\|h_{\mathcal{T}}\mathbf{u}\|_2\|(\mathbf{v}_h,q_h)\|_{\text{GLP}}.$$

The second term is handled by using the Cauchy–Schwarz inequality, trace inequality (2.4) and (2.9), as

$$\begin{aligned} \sum_{E\in\mathcal{E}_h^B}\int_E((\mathbf{u}-\mathbf{I}_h\mathbf{u})\cdot\mathbf{n})q_hds &\leq\left(\sum_{E\in\mathcal{E}_h^B}\frac{1}{h_E}\|(\mathbf{u}-\mathbf{I}_h\mathbf{u})\cdot\mathbf{n}\|_{L^2(E)}^2\right)^{\frac{1}{2}}\left(\sum_{E\in\mathcal{E}_h^B}h_E\|q_h\|_{L^2(E)}^2\right)^{\frac{1}{2}} \\ &\leq C\|h_{\mathcal{T}}\mathbf{u}\|_2\|(\mathbf{v}_h,q_h)\|_{\text{GLP}}. \end{aligned}$$

Using similar techniques as in the last term of Lemma 5 leads to

$$S_I(\mathbf{u}-\mathbf{I}_h\mathbf{u},\mathbf{v}_h)=[S_I(\mathbf{u}-\mathbf{I}_h\mathbf{u},\mathbf{u}-\mathbf{I}_h\mathbf{u})]^{\frac{1}{2}}[S_I(\mathbf{v}_h,\mathbf{v}_h)]^{\frac{1}{2}}\leq C\left\|h_{\mathcal{T}}^{\frac{3}{2}}\mathbf{u}\right\|\|(\mathbf{v}_h,q_h)\|_{\text{GLP}}.$$

The constant C in the above estimates depend on $\omega^{-1/2}$ and

$$S_B(\mathbf{u}-\mathbf{I}_h\mathbf{u},\mathbf{v}_h)=[S_B(\mathbf{u}-\mathbf{I}_h\mathbf{u},\mathbf{u}-\mathbf{I}_h\mathbf{u})]^{\frac{1}{2}}[S_B(\mathbf{v}_h,\mathbf{v}_h)]^{\frac{1}{2}}\leq\|h_{\mathcal{T}}\mathbf{u}\|_2\|(\mathbf{v}_h,q_h)\|_{\text{GLP}}.$$

The collection of all the above estimates shows (3.30) and this concludes the proof.

Lemma 7 Suppose $(\mathbf{u}, p) \in [H^2(\Omega)]^2 \times L_0^2(\Omega) \cap H^1(\Omega)$ and $(\mathbf{u}_h, p_h) \in \mathbf{V}_h \times \mathcal{Q}_h$ are the solutions to (2.2) and (3.14) respectively. Assume also that $\beta_E = \beta h_E$ for some $\beta > 0$ and let $(\mathbf{v}_h, q_h) \in \mathbf{V}_h \times \mathcal{Q}_h$. Then,

$$A_h((\mathbf{u} - \mathbf{u}_h, p - p_h), (\mathbf{v}_h, q_h)) \leq C \left(\|h_{\mathcal{T}} \mathbf{u}\|_2 + \|h_{\mathcal{T}} p\|_2 \right) \|(\mathbf{v}_h, q_h)\|_{\text{GLP}}. \quad (3.34)$$

Proof. Consider the model problem with the test function $(\mathbf{v}_h, q_h) \in \mathbf{V}_h \times \mathcal{Q}_h$. Using an integration by parts and the definition of the bilinear form,

$$a(\mathbf{u}, \mathbf{v}_h) - b(p, \mathbf{v}_h) + \sum_{E \in \mathcal{E}_h^B} \int_E (\mathbf{v}_h \cdot \mathbf{n}) p ds = (\mathbf{f}, \mathbf{v}_h) - \sum_{E \in \mathcal{E}_h^I} \int_E [\mathbf{v}_h \cdot \mathbf{n}] p ds.$$

Using the bilinear form (3.15) and the fact that $[\mathbf{u}] = 0$,

$$A_h((\mathbf{u} - \mathbf{u}_h, p - p_h), (\mathbf{v}_h, q_h)) = S_I(\mathbf{u}, \mathbf{v}_h) + \sum_{E \in \mathcal{E}_h^I} \int_E [\mathbf{v}_h \cdot \mathbf{n}] p ds. \quad (3.35)$$

In the first term of stabilization $S_I(\mathbf{u}, \mathbf{v}_h)$, applying the Cauchy–Schwarz inequality, Poincaré inequality (2.6) and $\beta_E \sim h_E$,

$$\begin{aligned} S_I(\mathbf{u}, \mathbf{v}_h) &= \sum_{E \in \mathcal{E}_h} \omega^{-1} \beta_E \int_{\mathcal{M}_E} \kappa_E (\nabla_h \cdot \mathbf{u}) \kappa_E (\nabla_h \cdot \mathbf{v}_h) dx \\ &\leq \left(\sum_{E \in \mathcal{E}_h} \omega^{-1} \beta_E \int_{\mathcal{M}_E} [\kappa_E (\nabla_h \cdot \mathbf{u})]^2 dx \right)^{\frac{1}{2}} \left(\sum_{E \in \mathcal{E}_h} \omega^{-1} \beta_E \int_{\mathcal{M}_E} [\kappa_E (\nabla_h \cdot \mathbf{v}_h)]^2 dx \right)^{\frac{1}{2}} \\ &\leq \left(\sum_{E \in \mathcal{E}_h} \omega^{-1} \beta_E \left\| \nabla_h \cdot \mathbf{u} - \frac{1}{|\mathcal{M}_E|} \int_{\mathcal{M}_E} \nabla_h \cdot \mathbf{u} dx \right\|_{L^2(\mathcal{M}_E)}^2 \right)^{1/2} \|(\mathbf{v}_h, q_h)\|_{\text{GLP}} \\ &\leq C \|h_{\mathcal{T}}^{3/2} \mathbf{u}\|_2 \|(\mathbf{v}_h, q_h)\|_{\text{GLP}}. \end{aligned}$$

The constant C in the above estimates depend on $\omega^{-1/2}$. The second term of (3.35) is handled by using the fact that the edge integral of the jump of $[\mathbf{v}_h \cdot \mathbf{n}]$ over each inner edge is zero and $\pi_h p$ is element-wise constant, i.e.,

$$\begin{aligned} \sum_{E \in \mathcal{E}_h^I} \int_E [\mathbf{v}_h \cdot \mathbf{n}] p ds &= \sum_{E \in \mathcal{E}_h^I} \int_E [\mathbf{v}_h \cdot \mathbf{n}] (p - \pi_h p) ds \leq \left(\sum_{E \in \mathcal{E}_h^I} \int_E h_E (p - \pi_h p)^2 ds \right)^{\frac{1}{2}} \left(\sum_{E \in \mathcal{E}_h^I} \int_E \frac{1}{h_E} [\mathbf{v}_h \cdot \mathbf{n}]^2 ds \right)^{\frac{1}{2}} \\ &\leq C \|h_{\mathcal{T}} p\|_1 \|(\mathbf{v}_h, q_h)\|_{\text{GLP}}. \end{aligned}$$

The collection of all the above estimates shows (3.34) and this concludes the proof.

Theorem 2 Let $(\mathbf{u}, p) \in [H^2(\Omega)]^2 \times L_0^2 \cap H^1(\Omega)$ and $(\mathbf{u}_h, p_h) \in \mathbf{V}_h \times \mathcal{Q}_h$ be the solutions to (2.2) and (3.14) respectively. Suppose $\beta_E = \beta h_E$ for some $\beta > 0$. Then it holds that

$$\|(\mathbf{u} - \mathbf{u}_h, p - p_h)\|_{\text{GLP}} \leq C \left(\|h_{\mathcal{T}} \mathbf{u}\|_2 + \|h_{\mathcal{T}} p\|_1 \right). \quad (3.36)$$

Proof. The triangle inequality implies that

$$\|(\mathbf{u} - \mathbf{u}_h, p - p_h)\|_{\text{GLP}} \leq \|(\mathbf{u} - \mathbf{I}_h \mathbf{u}, p - \pi_h p)\|_{\text{GLP}} + \|(\mathbf{I}_h \mathbf{u} - \mathbf{u}_h, \pi_h p - p_h)\|_{\text{GLP}}. \quad (3.37)$$

The first term of (3.37) follows from Lemma 5, i.e.,

$$\|(\mathbf{u} - \mathbf{I}_h \mathbf{u}, p - \pi_h p)\|_{\text{GLP}} \leq C \left(\|h_{\mathcal{T}} \mathbf{u}\|_2 + \|h_{\mathcal{T}} p\|_1 \right).$$

The second term of (3.37) is handled by using Theorem 1, as

$$\begin{aligned} \|(\mathbf{I}_h \mathbf{u} - \mathbf{u}_h, \pi_h p - p_h)\|_{\text{GLP}} &\leq 1/\gamma \sup_{(\mathbf{v}_h, q_h) \in \mathbf{V}_h \times Q_h} \frac{A_h((\mathbf{I}_h \mathbf{u} - \mathbf{u}_h, \pi_h p - p_h), (\mathbf{v}_h, q_h))}{\|(\mathbf{v}_h, q_h)\|_{\text{GLP}}} \\ &\leq 1/\gamma \sup_{(\mathbf{v}_h, q_h) \in \mathbf{V}_h \times Q_h} \frac{A_h(\mathbf{u} - \mathbf{u}_h, p - p_h), (\mathbf{v}_h, q_h)}{\|(\mathbf{v}_h, q_h)\|_{\text{GLP}}} \\ &\quad + \sup_{(\mathbf{v}_h, q_h) \in \mathbf{V}_h \times Q_h} \frac{A_h((\mathbf{I}_h \mathbf{u} - \mathbf{u}, \pi_h p - p), (\mathbf{v}_h, q_h))}{\|(\mathbf{v}_h, q_h)\|_{\text{GLP}}}. \end{aligned} \quad (3.38)$$

Finally, the result follows by using Lemma 6 and Lemma 7 in (3.38) and this concludes the proof.

4 Piecewise linear nonconforming approximation of pressure ($[\mathbb{P}_1^{nc}(\mathcal{T}_h)]^2 / \mathbb{P}_1^{nc}(\mathcal{T}_h)$)

Consider the vector spaces

$$\mathbf{V}_h := [\mathbb{P}_1^{nc}(\mathcal{T}_h)]^2, \quad \mathbf{V}_h^0 := [\mathbb{P}_{1,0}^{nc}(\mathcal{T}_h)]^2 \quad \text{and} \quad Q_h := \mathbb{P}_1^{nc}(\mathcal{T}_h) \cap L_0^2(\Omega).$$

This section deals with piecewise linear space for pressure discretization to better estimate the pressure and get the optimal order of convergence for the velocity approximation. But with this choice of pressure, the inf-sup compatibility between the velocity and pressure discrete spaces are lost. Thus, in addition to stabilization for consistency error, more stabilization terms are required to control the incompressibility condition, which makes discretization inf-sup stable, and can handle discontinuity of pressure along the edges [4, 35].

The generalized local projection stabilized discrete form with ($[\mathbb{P}_1^{nc}]^2 / \mathbb{P}_1^{nc}$) reads as: Find $(\mathbf{u}_h, p_h) \in \mathbf{V}_h \times Q_h$ such that

$$A_h((\mathbf{u}_h, p_h), (\mathbf{v}, q)) = l(\mathbf{v}, q) \quad \text{for all } (\mathbf{v}, q) \in \mathbf{V}_h \times Q_h, \quad (4.39)$$

where

$$A_h((\mathbf{u}_h, p_h), (\mathbf{v}, q)) = a_h(\mathbf{u}_h, \mathbf{v}) - b_h(p_h, \mathbf{v}) + b_h(q, \mathbf{u}_h) + S_h((\mathbf{u}_h, p_h), (\mathbf{v}, q)),$$

and

$$\begin{aligned}
a_h(\mathbf{u}_h, \mathbf{v}) &:= \sum_{K \in \mathcal{T}_h} \int_K \boldsymbol{\omega}^{-1}(\mathbf{u}_h \cdot \mathbf{v}) dx, \\
b_h(q, \mathbf{u}_h) &:= (q, \nabla_h \cdot \mathbf{u}_h) - \sum_{E \in \mathcal{E}_h^B} \int_E (\mathbf{u}_h \cdot \mathbf{n}) q ds - \sum_{E \in \mathcal{E}_h^I} \int_E [\mathbf{u}_h \cdot \mathbf{n}] \{q\} ds, \\
S_h((\mathbf{u}_h, p_h), (\mathbf{v}, q)) &:= S_{\mathbf{u}}(\mathbf{u}_h, \mathbf{v}) + S_p(p_h, q), \\
S_{\mathbf{u}}(\mathbf{u}_h, \mathbf{v}) &:= \sum_{E \in \mathcal{E}_h} \boldsymbol{\omega}^{-1} \beta_E (\boldsymbol{\kappa}_E (\nabla_h \cdot \mathbf{u}_h), \boldsymbol{\kappa}_E (\nabla_h \cdot \mathbf{v}))_{L^2(\mathcal{M}_E)} + \sum_{E \in \mathcal{E}_h} \int_E [\mathbf{u}_h \cdot \mathbf{n}] [\mathbf{v} \cdot \mathbf{n}] ds, \\
S_p(p_h, q) &:= \sum_{E \in \mathcal{E}_h} \boldsymbol{\omega} \beta_E (\boldsymbol{\kappa}_E (\nabla_h p_h), \boldsymbol{\kappa}_E (\nabla_h q))_{L^2(\mathcal{M}_E)} + \sum_{E \in \mathcal{E}_h^I} \int_E [p_h] [q] ds, \\
l(\mathbf{v}, q) &:= (\mathbf{f}, \mathbf{v}) + (\phi, q) + \sum_{E \in \mathcal{E}_h^B} \left(- \int_E \psi q ds + \int_E \frac{\Psi}{h_E} (\mathbf{v} \cdot \mathbf{n}) ds \right).
\end{aligned}$$

Further, the GLP norm for $\mathbf{V}_h \times Q_h$ is denoted by

$$\|(\mathbf{u}_h, p_h)\|_{\text{GLP}}^2 := \left\| \boldsymbol{\omega}^{-\frac{1}{2}} \mathbf{u}_h \right\|^2 + \|h^{\frac{1}{2}}_{\mathcal{T}_h} (\nabla_h \cdot \mathbf{u}_h)\|^2 + \|p_h\|^2 + S_h((\mathbf{u}_h, p_h), (\mathbf{u}_h, p_h)). \quad (4.40)$$

4.1 Stability

In addition, the key statement of this article is the following theorem, which guarantees that the discrete bilinear form (4.39) is well-posed.

Theorem 3 *Suppose $\beta_E = \beta h_E$ for some $\beta > 0$. Then, the finite element formulation (4.39) satisfies the following inf-sup condition for some positive constant ν , independent of h :*

$$\inf_{(\mathbf{u}_h, p_h) \in \mathbf{V}_h \times Q_h} \sup_{(\mathbf{v}_h, q_h) \in \mathbf{V}_h \times Q_h} \frac{A_h((\mathbf{u}_h, p_h), (\mathbf{v}_h, q_h))}{\|(\mathbf{u}_h, p_h)\|_{\text{GLP}} \|(\mathbf{v}_h, q_h)\|_{\text{GLP}}} \geq \nu.$$

Proof. First, consider the test function pair $(\mathbf{v}_h, q_h) = (\mathbf{u}_h, p_h)$. Then,

$$A_h((\mathbf{u}_h, p_h), (\mathbf{u}_h, p_h)) = \left\| \boldsymbol{\omega}^{-\frac{1}{2}} \mathbf{u}_h \right\|^2 + S_h((\mathbf{u}_h, p_h), (\mathbf{u}_h, p_h)).$$

The stability of the pair $([H_0^1(\Omega)]^2 / L_0^2(\Omega))$ [25] implies that there exists a constant $\alpha > 0$ such that

$$\inf_{q_h \in Q_h} \sup_{\mathbf{v} \in [H_0^1(\Omega)]^2} \frac{(\text{div } \mathbf{v}, q_h)}{\|\nabla \mathbf{v}\| \|q_h\|} \geq \alpha > 0. \quad (4.41)$$

As a consequence of (4.41), for each $p_h \in Q_h$, there exists $\mathbf{z} \in H_0^1(\Omega)^2$ such that

$$-(\nabla_h \cdot \mathbf{z}, p_h) = \|p_h\|^2 \text{ and } \|\mathbf{z}\|_1 \leq C_1 \|p_h\|. \quad (4.42)$$

Let $\mathbf{z} \in H_0^1(\Omega)^2$ be defined as in (4.42). Let $\mathbf{z}_h = \mathbf{I}_h \mathbf{z} \in \mathbf{V}_h$. Then, by choosing $(\mathbf{v}_h, q_h) = (\mathbf{z}_h, 0)$ in (4.39),

$$A_h((\mathbf{u}_h, p_h), (\mathbf{z}_h, 0)) = a_h(\mathbf{u}_h, \mathbf{z}_h) - b_h(p_h, \mathbf{z}_h) + S_h((\mathbf{u}_h, p_h), (\mathbf{z}_h, 0)). \quad (4.43)$$

Most of the estimates for the right-hand side terms of (4.43) follow from (3.21). Only those estimates that are new or different from (3.21) are discussed here. In the second term of (4.43), add $0 = (p_h, p_h) - (p_h, -\nabla_h \cdot \mathbf{z})$ to obtain

$$\begin{aligned} -b_h(p_h, \mathbf{z}_h) &= -(p_h, \nabla_h \cdot \mathbf{z}_h) + \sum_{E \in \mathcal{E}_h^I} \int_E [\mathbf{z}_h \cdot \mathbf{n}] \{p_h\} ds + \sum_{E \in \mathcal{E}_h^B} \int_E (\mathbf{z}_h \cdot \mathbf{n}) p_h ds \\ &= \|p_h\|^2 + (p_h, \nabla_h \cdot (\mathbf{z} - \mathbf{z}_h)) + \sum_{E \in \mathcal{E}_h^I} \int_E [\mathbf{z}_h \cdot \mathbf{n}] \{p_h\} ds + \sum_{E \in \mathcal{E}_h^B} \int_E (\mathbf{z}_h \cdot \mathbf{n}) p_h ds. \end{aligned} \quad (4.44)$$

Applying an integration by parts to the second term of (4.44),

$$\begin{aligned} (p_h, \nabla_h \cdot (\mathbf{z} - \mathbf{z}_h)) &= -(\nabla_h p_h, (\mathbf{z} - \mathbf{z}_h)) + \sum_{E \in \mathcal{E}_h^I} \int_E \{p_h\} [(\mathbf{z} - \mathbf{z}_h) \cdot \mathbf{n}] ds \\ &\quad + \sum_{E \in \mathcal{E}_h^I} \int_E [p_h] \{(\mathbf{z} - \mathbf{z}_h) \cdot \mathbf{n}\} ds + \sum_{E \in \mathcal{E}_h^B} \int_E p_h ((\mathbf{z} - \mathbf{z}_h) \cdot \mathbf{n}) ds. \end{aligned}$$

It follows that

$$-b_h(p_h, \mathbf{z}_h) = \|p_h\|^2 - (\nabla_h p_h, \mathbf{z} - \mathbf{z}_h) + \sum_{E \in \mathcal{E}_h^I} \int_E [p_h] \{(\mathbf{z} - \mathbf{z}_h) \cdot \mathbf{n}\} ds. \quad (4.45)$$

Use the canonical Crouzeix–Raviart edge basis-function ϕ_E at the edge $E \in \mathcal{E}_h$ over the mesh \mathcal{T}_h . Since, $\sum_{E \in \mathcal{E}_h} \phi_E \equiv 1$,

$$(\nabla_h p_h, \mathbf{z} - \mathbf{z}_h) = \sum_{K \in \mathcal{T}_h} \int_K \nabla_h p_h (\mathbf{z} - \mathbf{z}_h) \sum_{E \in \mathcal{E}_h} \phi_E dx = \sum_{E \in \mathcal{E}_h} \int_{\mathcal{M}_E} (\mathbf{z} - \mathbf{z}_h) \nabla_h p_h \phi_E dx. \quad (4.46)$$

Using the orthogonality of L^2 -projection with the test function $C_E \phi_E \in \mathbf{V}_h$, where $C_E = \frac{1}{|\mathcal{M}_E|} \int_{\mathcal{M}_E} \nabla_h p_h dx$ and $\|\phi\|_\infty \leq 1$,

$$\begin{aligned} (\nabla_h p_h, \mathbf{z} - \mathbf{z}_h) &= \sum_{E \in \mathcal{E}_h} \int_{\mathcal{M}_E} (\mathbf{z} - \mathbf{z}_h) \left(\nabla_h p_h - \frac{1}{|\mathcal{M}_E|} \int_{\mathcal{M}_E} \nabla_h p_h dx \right) \phi_E dx \\ &\leq \left(\sum_{E \in \mathcal{E}_h} \int_{\mathcal{M}_E} \omega^{-1} \beta_E^{-1} (\mathbf{z} - \mathbf{z}_h)^2 dx \right)^{\frac{1}{2}} \left(\sum_{E \in \mathcal{E}_h} \int_{\mathcal{M}_E} \omega \beta_E \kappa_E^2 (\nabla_h p_h) dx \right)^{\frac{1}{2}} \\ &\leq \frac{1}{8} \|p_h\|^2 + CS_h((\mathbf{u}_h, p_h), (\mathbf{u}_h, p_h)). \end{aligned}$$

The constant C in the above estimates depend on $\omega^{-1/2}$. The last term of (4.45) is estimated by using trace inequality, as

$$\begin{aligned} \sum_{E \in \mathcal{E}_h^I} \int_E [p_h] \{(\mathbf{z} - \mathbf{z}_h) \cdot \mathbf{n}\} ds &\leq \left(\sum_{E \in \mathcal{E}_h^I} \| [p_h] \|_{L^2(E)}^2 \right)^{\frac{1}{2}} \left(\sum_{E \in \mathcal{E}_h^I} \| \{(\mathbf{z} - \mathbf{z}_h) \cdot \mathbf{n}\} \|_{L^2(E)}^2 \right)^{\frac{1}{2}} \\ &\leq \frac{1}{8} \|p_h\|^2 + \sum_{E \in \mathcal{E}_h^I} \int_E [p_h]^2 ds. \end{aligned}$$

Put together, (4.43) leads to

$$A_h((\mathbf{u}_h, p_h), (\mathbf{z}_h, 0)) \geq \frac{1}{2} \|p_h\|^2 - C \left(\|\mathbf{u}_h\|^2 + \frac{1}{2} S_h((\mathbf{u}_h, p_h), (\mathbf{u}_h, p_h)) \right).$$

Finally, the control of $\left\| h^{\frac{1}{2}}_{\mathcal{T}} (\nabla_h \cdot \mathbf{u}_h) \right\|^2$ can be obtained by choosing $(\mathbf{v}_h, q_h) = (0, h_{\mathcal{T}} (\nabla_h \cdot \mathbf{u}_h))$ in (4.39), that is,

$$A_h((\mathbf{u}_h, p_h), (0, I_h(h_{\mathcal{T}} (\nabla_h \cdot \mathbf{u}_h)))) = b_h(I_h(h_{\mathcal{T}} (\nabla_h \cdot \mathbf{u}_h)), \mathbf{u}_h) + S_h((\mathbf{u}_h, p_h), (0, I_h(h_{\mathcal{T}} (\nabla_h \cdot \mathbf{u}_h))). \quad (4.47)$$

By adding and subtracting $\left\| h^{\frac{1}{2}}_{\mathcal{T}} (\nabla_h \cdot \mathbf{u}_h) \right\|^2$ in the first term of (4.47),

$$\begin{aligned} b_h(I_h(h_{\mathcal{T}} (\nabla_h \cdot \mathbf{u}_h)), \mathbf{u}_h) &= \left\| h^{\frac{1}{2}}_{\mathcal{T}} (\nabla_h \cdot \mathbf{u}_h) \right\|^2 + (I_h(h_{\mathcal{T}} (\nabla_h \cdot \mathbf{u}_h)) - h_{\mathcal{T}} (\nabla_h \cdot \mathbf{u}_h), \nabla_h \cdot \mathbf{u}_h) \\ &\quad - \sum_{E \in \mathcal{E}_h^B} \int_E (\mathbf{u}_h \cdot \mathbf{n}) I_h(h_{\mathcal{T}} (\nabla_h \cdot \mathbf{u}_h)) ds - \sum_{E \in \mathcal{E}_h^I} \int_E [\mathbf{u}_h \cdot \mathbf{n}] \{I_h(h_{\mathcal{T}} (\nabla_h \cdot \mathbf{u}_h))\} ds. \end{aligned} \quad (4.48)$$

The second term of (4.48) is estimated as

$$\begin{aligned} &(I_h(h_{\mathcal{T}} (\nabla_h \cdot \mathbf{u}_h)) - h_{\mathcal{T}} (\nabla_h \cdot \mathbf{u}_h), \nabla_h \cdot \mathbf{u}_h) \\ &= \sum_{E \in \mathcal{M}_E} \int_{\mathcal{M}_E} (I_h(h_K (\nabla_h \cdot \mathbf{u}_h)) - h_K (\nabla_h \cdot \mathbf{u}_h)) \left(\nabla_h \cdot \mathbf{u}_h - \frac{1}{|\mathcal{M}_E|} \int_{\mathcal{M}_E} \nabla_h \cdot \mathbf{u}_h dx \right) \phi_E dx \\ &\leq \left(\sum_{E \in \mathcal{M}_E} \omega \beta_E^{-1} \|I_h(h_{\mathcal{T}} (\nabla_h \cdot \mathbf{u}_h)) - h_{\mathcal{T}} (\nabla_h \cdot \mathbf{u}_h)\|_{L^2(\mathcal{M}_E)}^2 \right)^{\frac{1}{2}} [S_h((\mathbf{u}_h, 0), (\mathbf{u}_h, 0))]^{\frac{1}{2}} \\ &\leq \frac{1}{8} \left\| h^{\frac{1}{2}}_{\mathcal{T}} (\nabla_h \cdot \mathbf{u}_h) \right\|^2 + \frac{C}{4} S_h((\mathbf{u}_h, p_h), (\mathbf{u}_h, q_h)). \end{aligned}$$

The constant C in the above estimates depend on $\omega^{1/2}$. The third term of (4.48) is handled by applying the Cauchy–Schwarz inequality, trace inequality, stability property of projection operator (2.11) and Young’s inequality, as

$$\begin{aligned} \sum_{E \in \mathcal{E}_h^B} \int_E (\mathbf{u}_h \cdot \mathbf{n}) I_h(h_K (\nabla_h \cdot \mathbf{u}_h)) ds &\leq \left(\sum_{E \in \mathcal{E}_h^B} \int_E (\mathbf{u}_h \cdot \mathbf{n})^2 ds \right)^{\frac{1}{2}} \left(\sum_{E \in \mathcal{E}_h^B} \int_E (I_h(h_K (\nabla_h \cdot \mathbf{u}_h))^2 ds \right)^{\frac{1}{2}} \\ &\leq \frac{1}{8} \left\| h^{\frac{1}{2}}_{\mathcal{T}} (\nabla_h \cdot \mathbf{u}_h) \right\|^2 + \frac{C}{8} S_h((\mathbf{u}_h, 0), (\mathbf{u}_h, 0)). \end{aligned}$$

In a similar way, the last term of (4.48) is handled as

$$\begin{aligned} \sum_{E \in \mathcal{E}_h^I} \int_E [\mathbf{u}_h \cdot \mathbf{n}] \{I_h(h_K(\nabla_h \cdot \mathbf{u}_h))\} ds &\leq \left(\sum_{E \in \mathcal{E}_h^I} \int_E [\mathbf{u}_h \cdot \mathbf{n}]^2 ds \right)^{\frac{1}{2}} \left(\sum_{E \in \mathcal{E}_h^I} \int_E \{I_h(h_K(\nabla_h \cdot \mathbf{u}_h))\}^2 ds \right)^{\frac{1}{2}} \\ &\leq \frac{1}{8} \left\| h_{\mathcal{T}}^{\frac{1}{2}}(\nabla_h \cdot \mathbf{u}_h) \right\|^2 + \frac{C}{8} S_h((\mathbf{u}_h, 0), (\mathbf{u}_h, 0)). \end{aligned}$$

The last term of (4.47) is handled by using the Cauchy–Schwarz inequality, boundedness of the local projection operator, inverse inequality, the stability of the projection operator and Young’s inequality,

$$\begin{aligned} S_h((\mathbf{u}_h, p_h), (0, I_h(h_{\mathcal{T}}(\nabla_h \cdot \mathbf{u}_h)))) &\leq S_h((\mathbf{u}_h, p_h), (\mathbf{u}_h, p_h))^{\frac{1}{2}} S_h((0, I_h(h_{\mathcal{T}}(\nabla_h \cdot \mathbf{u}_h)), (0, I_h(h_{\mathcal{T}}(\nabla_h \cdot \mathbf{u}_h))))^{\frac{1}{2}} \\ &\leq \frac{1}{8} \left\| h_{\mathcal{T}}^{\frac{1}{2}}(\nabla_h \cdot \mathbf{u}_h) \right\|^2 + \frac{C}{4} S_h((\mathbf{u}_h, p_h), (\mathbf{u}_h, p_h)). \end{aligned}$$

The constant C in the above estimates depend on ω . Put together, (4.47) leads to

$$A_h((\mathbf{u}_h, p_h), (0, I_h(h_{\mathcal{T}}(\nabla_h \cdot \mathbf{u}_h)))) \geq \frac{1}{2} \left\| h_{\mathcal{T}}^{\frac{1}{2}}(\nabla_h \cdot \mathbf{u}_h) \right\|^2 - \frac{C}{2} S_h((\mathbf{u}_h, p_h), (\mathbf{u}_h, p_h)).$$

The selection of (\mathbf{v}_h, q_h) is

$$(\mathbf{v}_h, q_h) = (\mathbf{u}_h, p_h) + \frac{1}{C+1} (\mathbf{z}_h, 0) + \frac{1}{C+1} (0, I_h(h_{\mathcal{T}} \nabla_h \cdot \mathbf{u}_h)),$$

where I_h is defined in (2.7). Finally, the rest of the proof follows in a similar way as in Theorem 1.

4.2 *A priori* error estimates

This subsection discusses *a priori* error estimates for $[\mathbb{P}_1^{nc}(\mathcal{T}_h)]^2 / \mathbb{P}_1^{nc}(\mathcal{T}_h)$ approximation for the velocity–pressure pair with respect to the GLP norm.

Lemma 8 *Suppose $\beta_E = \beta h_E$ for some $\beta > 0$. Let $(\mathbf{u}, q) \in [\mathbf{H}^2(\Omega)]^2 \times \mathbf{L}_0^2(\Omega) \cap \mathbf{H}^2(\Omega)$. Then,*

$$\|(\mathbf{u} - \mathbf{I}_h \mathbf{u}, p - I_h p)\|_{\text{GLP}} \leq C \left(\left\| h_{\mathcal{T}}^{\frac{3}{2}} \mathbf{u} \right\|_2 + \left\| h_{\mathcal{T}}^{\frac{3}{2}} p \right\|_2 \right).$$

Proof. The idea of the proof is same as for the proof of Lemma 5. Following a similar argument, the proof can be derived.

Lemma 9 *Suppose $\beta_E = \beta h_E$ for some $\beta > 0$. Let $(\mathbf{u}, p) \in [\mathbf{H}^2(\Omega)]^2 \times \mathbf{L}_0^2 \cap \mathbf{H}^2(\Omega)$ and for all $(\mathbf{v}_h, q_h) \in \mathbf{V}_h \times \mathbf{Q}_h$. Then,*

$$A_h((\mathbf{u} - \mathbf{I}_h \mathbf{u}, p - I_h p), (\mathbf{v}_h, q_h)) \leq C \left(\left\| h_{\mathcal{T}}^{\frac{3}{2}} \mathbf{u} \right\|_2 + \left\| h_{\mathcal{T}}^{\frac{3}{2}} p \right\|_2 \right) \|(\mathbf{v}_h, q_h)\|_{\text{GLP}}. \quad (4.49)$$

Proof. Consider the bilinear form (4.39):

$$\begin{aligned} A_h((\mathbf{u}-\mathbf{I}_h\mathbf{u}, p-I_h p), (\mathbf{v}_h, q_h)) &= a_h(\mathbf{u}-\mathbf{I}_h\mathbf{u}, \mathbf{v}_h) - b_h(p-I_h p, \mathbf{v}_h) + b_h(q_h, \mathbf{u}-\mathbf{I}_h\mathbf{u}) \\ &\quad + S_h((\mathbf{u}-\mathbf{I}_h\mathbf{u}, p-I_h p), (\mathbf{v}_h, q_h)). \end{aligned} \quad (4.50)$$

The first term of (4.50) can be handled as in Lemma 6. Consider the second term of (4.50):

$$b_h(p-I_h p, \mathbf{v}_h) = (p-I_h p, \nabla_h \cdot \mathbf{v}_h) - \sum_{E \in \mathcal{E}_h^R} \int_E (\mathbf{v}_h \cdot \mathbf{n}) (p-I_h p) ds - \sum_{E \in \mathcal{E}_h^I} \int_E [\mathbf{v}_h \cdot \mathbf{n}] \{p-I_h p\} ds. \quad (4.51)$$

The first term of (4.51) is handled by using the Cauchy–Schwarz inequality and (2.7), as

$$(p-I_h p, \nabla_h \cdot \mathbf{v}_h) \leq \|p-I_h p\| \|\nabla_h \cdot \mathbf{v}_h\| \leq \left\| h_{\mathcal{T}}^{\frac{3}{2}} p \right\|_2 \|\mathbf{v}_h, q_h\|_{\text{GLP}}.$$

The estimates for the second term of (4.51) follows from Lemma 6. Applying the Cauchy–Schwarz inequality in the last term of (4.51),

$$\sum_{E \in \mathcal{E}_h^I} \int_E [\mathbf{v}_h \cdot \mathbf{n}] \{p-I_h p\} ds \leq \left(\sum_{E \in \mathcal{E}_h^I} \|\mathbf{v}_h \cdot \mathbf{n}\|_{L^2(E)}^2 \right)^{\frac{1}{2}} \left(\sum_{E \in \mathcal{E}_h^I} \|\{p-I_h p\}\|_{L^2(E)}^2 \right)^{\frac{1}{2}}.$$

At the edge E , the average term has contribution for both the triangles sharing that edge. Using the trace inequality (2.3),

$$\|\{p-I_h p\}\|_{L^2(E)} \leq C \left(h_K^{-1/2} \|p-I_h p\|_{L^2(\mathcal{M}_E)} + h_K^{1/2} \|\nabla_h(p-I_h p)\|_{L^2(\mathcal{M}_E)} \right).$$

Squaring and summing up all the inner edges and using (2.8),

$$\sum_{E \in \mathcal{E}_h^I} \int_E [\mathbf{v}_h \cdot \mathbf{n}] \{p-I_h p\} ds \leq \left\| h_{\mathcal{T}}^{\frac{3}{2}} p \right\|_2 \|\mathbf{v}_h, q_h\|_{\text{GLP}}.$$

Applying an integration by parts in the next term of the bilinear form (4.50),

$$b_h(\mathbf{u}-\mathbf{I}_h\mathbf{u}, q_h) = -(\nabla_h q_h, \mathbf{u}-\mathbf{I}_h\mathbf{u}) + \sum_{E \in \mathcal{E}_h^I} \int_E \{(\mathbf{u}-\mathbf{I}_h\mathbf{u}) \cdot \mathbf{n}\} [q_h] ds. \quad (4.52)$$

Using a similar technique as in (4.46), the first term of (4.52) is estimated as

$$\begin{aligned} (\nabla_h q_h, \mathbf{u}-\mathbf{I}_h\mathbf{u}) &= \sum_{E \in \mathcal{E}_h^I} \int_{\mathcal{M}_E} (\mathbf{u}-\mathbf{I}_h\mathbf{u}) \left(\nabla_h q_h - \frac{1}{|\mathcal{M}_E|} \int_{\mathcal{M}_E} \nabla_h q_h dx \right) \phi_E dx \\ &\leq \left(\sum_{E \in \mathcal{E}_h^I} \int_{\mathcal{M}_E} \omega^{-1} \beta_E^{-1} (\mathbf{u}-\mathbf{I}_h\mathbf{u})^2 dx \right)^{\frac{1}{2}} \left(\sum_{E \in \mathcal{E}_h^I} \int_{\mathcal{M}_E} \omega \beta_E \kappa_E^2 (\nabla_h q_h) dx \right)^{\frac{1}{2}} \\ &\leq C \left\| h_{\mathcal{T}}^{\frac{3}{2}} \mathbf{u} \right\|_2 \|\mathbf{v}_h, q_h\|_{\text{GLP}}. \end{aligned}$$

The constant C in the above estimates depend on $\omega^{-1/2}$. Using (2.3) and (2.8),

$$\sum_{E \in \mathcal{E}_h^I} \int_E \{(\mathbf{u} - \mathbf{I}_h \mathbf{u}) \cdot \mathbf{n}\} [q_h] ds \leq C \left\| h^{\frac{3}{2}} \mathbf{u} \right\|_2 \|\!(\mathbf{v}_h, q_h)\!\|_{\text{GLP}}.$$

In the stabilization terms, applying the Cauchy–Schwarz inequality, boundedness of the local projection operator and (2.7)–(2.8),

$$\begin{aligned} S_h((\mathbf{u} - \mathbf{I}_h \mathbf{u}, p - I_h p), (\mathbf{v}_h, q_h)) &= [S_h((\mathbf{u} - \mathbf{I}_h \mathbf{u}, p - I_h p), (\mathbf{u} - \mathbf{I}_h \mathbf{u}, p - I_h p))]^{\frac{1}{2}} [S_h((\mathbf{v}_h, q_h), (\mathbf{v}_h, q_h))]^{\frac{1}{2}} \\ &\leq C \left(C_1 \left\| h^{\frac{3}{2}} \mathbf{u} \right\|_2 + C_2 \left\| h^{\frac{3}{2}} p \right\|_2 \right) \|\!(\mathbf{v}_h, q_h)\!\|_{\text{GLP}}. \end{aligned}$$

The constants C_1 and C_2 in the above estimates depend on $\omega^{-1/2}$ and $\omega^{1/2}$, respectively. The last two terms of the bilinear form are estimated as

$$\begin{aligned} \sum_{E \in \mathcal{E}_h} \int_E [(\mathbf{u} - \mathbf{I}_h \mathbf{u}) \cdot \mathbf{n}] [\mathbf{v}_h \cdot \mathbf{n}] ds &\leq \left\| h^{\frac{3}{2}} \mathbf{u} \right\|_2 \|\!(\mathbf{v}_h, q_h)\!\|_{\text{GLP}}, \\ \sum_{E \in \mathcal{E}_h^I} \int_E [p - I_h p] [q_h] ds &\leq \left\| h^{\frac{3}{2}} p \right\|_2 \|\!(\mathbf{v}_h, q_h)\!\|_{\text{GLP}}. \end{aligned}$$

The combination of all the above estimates shows (4.49) and this concludes the proof.

Lemma 10 *Suppose $\beta_E = \beta h_E$ for some $\beta > 0$. Let $(\mathbf{u}, p) \in [\mathbf{H}^2(\Omega)]^2 \times \mathbf{L}_0^2(\Omega) \cap \mathbf{H}^2(\Omega)$ and $(\mathbf{u}_h, p_h) \in \mathbf{V}_h \times Q_h$ be the solutions to (2.2) and (4.39) respectively. For any $(\mathbf{v}_h, q_h) \in \mathbf{V}_h \times Q_h$, it holds that*

$$A_h((\mathbf{u} - \mathbf{u}_h, p - p_h), (\mathbf{v}_h, q_h)) \leq C \left(\left\| h^{\frac{3}{2}} \mathbf{u} \right\|_2 + \left\| h^{\frac{3}{2}} p \right\|_2 \right) \|\!(\mathbf{v}_h, q_h)\!\|_{\text{GLP}}. \quad (4.53)$$

Proof. The model problem with the test function $(\mathbf{v}_h, q_h) \in \mathbf{V}_h \times Q_h$, definition of the bilinear form and the fact that $[\mathbf{u}] = 0$ and $[p] = 0$ across edges leads to

$$A_h((\mathbf{u} - \mathbf{u}_h, p - p_h), (\mathbf{v}_h, q_h)) = \sum_{E \in \mathcal{E}_h} \omega^{-1} \beta_E \int_{\mathcal{M}_E} \kappa_E (\nabla_h \cdot \mathbf{u}) \kappa_E (\nabla_h \cdot \mathbf{v}_h) dx + \sum_{E \in \mathcal{E}_h} \omega \beta_E \int_{\mathcal{M}_E} \kappa_E (\nabla_h p) \kappa_E (\nabla_h q_h) dx. \quad (4.54)$$

In the first term on the right-hand side of (4.54), using the Cauchy–Schwarz inequality, Poincaré inequality and $\beta_E \sim h_E$,

$$\begin{aligned} &\sum_{E \in \mathcal{E}_h} \omega^{-1} \beta_E \int_{\mathcal{M}_E} \kappa_E (\nabla_h \cdot \mathbf{u}) \kappa_E (\nabla_h \cdot \mathbf{v}_h) dx \\ &\leq \left(\sum_{E \in \mathcal{E}_h} \omega^{-1} \beta_E \left\| \nabla_h \cdot \mathbf{u} - \frac{1}{|\mathcal{M}_E|} \int_{\mathcal{M}_E} \nabla_h \cdot \mathbf{u} dx \right\|_{\mathbf{L}^2(\mathcal{M}_E)}^2 \right)^{\frac{1}{2}} \left(\sum_{E \in \mathcal{E}_h} \omega^{-1} \beta_E \int_{\mathcal{M}_E} \kappa_E^2 (\nabla_h \cdot \mathbf{v}_h) dx \right)^{\frac{1}{2}} \\ &\leq C \left\| h^{\frac{3}{2}} \mathbf{u} \right\|_2 \|\!(\mathbf{v}_h, q_h)\!\|_{\text{GLP}}. \end{aligned}$$

The constant C in the above estimates depend on $\omega^{-1/2}$. In a similar way, the second term can be estimated as

$$\sum_{E \in \mathcal{E}_h} \omega \beta_E \int_{\mathcal{M}_E} \kappa_E (\nabla_h p) \kappa_E (\nabla_h q_h) dx \leq C \left\| h_{\mathcal{T}}^{3/2} p \right\|_2 \left\| (\mathbf{v}_h, q_h) \right\|_{\text{GLP}}.$$

The constant C in the above estimate depending on $\omega^{1/2}$. The collection of all the above estimates shows (4.53) and this concludes the proof.

Theorem 4 *Let $(\mathbf{u}, p) \in [\mathbf{H}^2(\Omega)]^2 \times L_0^2(\Omega) \cap \mathbf{H}^2(\Omega)$ and $(\mathbf{u}_h, p_h) \in \mathbf{V}_h \times Q_h$ be the solutions to (2.2) and (3.14) respectively. Assume that $\beta_E = \beta h_E$ for some $\beta > 0$. Then it holds that*

$$\left\| (\mathbf{u} - \mathbf{u}_h, p - p_h) \right\|_{\text{GLP}} \leq C \left(\left\| h_{\mathcal{T}}^{\frac{3}{2}} \mathbf{u} \right\|_2 + \left\| h_{\mathcal{T}}^{\frac{3}{2}} p \right\|_2 \right).$$

Proof. This follows from the combination of Lemma 9 and Lemma 10, as in the proof of Theorem 2.

5 Numerical results

In this section, an array of numerical results is presented to illustrate the derived theoretical estimates. The numerical solutions of all examples are computed on hierarchy of uniformly-refined triangular meshes having 16, 64, 256, 1024 and 4096 elements. The initial and an uniformly-refined mesh are shown in Figure 2.

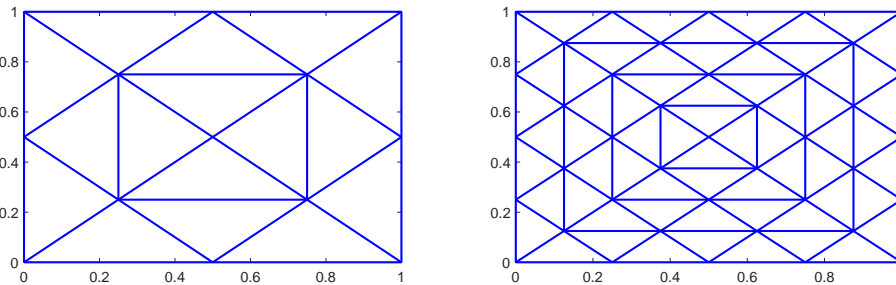


Fig. 2 Triangulations used for computations in section 5.

Example: Consider the model problem (2.1) in $\Omega = (0,1)^2$ with a given exact solution:

$$\begin{aligned} \mathbf{u}(x,y) &= (-2\pi \sin(2\pi x) \cos(2\pi y), 2\pi \cos(2\pi x) \sin(2\pi y)), \\ p(x,y) &= \sin(2\pi x) \sin(2\pi y). \end{aligned}$$

The numerical tests for the Darcy equations are conducted with approximations of $\mathbb{P}_1^{nc} / \mathbb{P}_0$ and $\mathbb{P}_1^{nc} / \mathbb{P}_1^{nc}$. Set the stabilization parameters $\beta_E = \beta h_E$ with $\beta = 1$ in the finite element formulations (3.14) and (4.39). The GLPS finite element system offers a non-oscillatory solution and hence, it supports the proposed stabilized schemes. The Figure 3 shows the GLPS FEM solutions $\mathbb{P}_1^{nc} / \mathbb{P}_0$ approximation

with 6208 number of degrees of freedom for the unknown (\mathbf{u}_h, p_h) with $(\omega=1)$. The errors are measured in the L^2 - norm, H^1 -seminorm and GLP norm. The orders of convergence are computed for the errors obtained with the two finest meshes. The effect of parameters \varkappa and λ on the rates of convergence is also investigated. The Tables 1 and 2 show the errors and order of convergence for $(\mathbb{P}_1^{nc}/\mathbb{P}_0)$ finite element solutions of the model problem with $(\omega=1)$ and $(\omega=0.1)$ respectively. A second-order convergence can be observed in the L^2 -norm and a first-order convergence in the H^1 -seminorm. Moreover, the convergence order one was obtained with respect to the GLP norm as defined in (3.16). In addition, the Figure 4 shows the convergence behaviour of $\mathbb{P}_1^{nc}/\mathbb{P}_0$ approximation of the Darcy equations with respect to the L^2 -norm, H^1 -norm and GLP norm with $(\omega=1)$ and $(\omega=0.1)$; it confirms the expected rate of convergence.

It is reported that the velocity and pressure approximation pair $\mathbb{P}_1^{nc}/\mathbb{P}_1^{nc}$ is not inf-sup stable for the Darcy flow problem. The GLP stabilization works effectively for the $\mathbb{P}_1^{nc}/\mathbb{P}_1^{nc}$ approximation. The GLP formulation (4.39) overcomes the space incompatibility issue and improves the pressure's approximation. The Figure 5 shows the GLPS FEM solutions $\mathbb{P}_1^{nc}/\mathbb{P}_1^{nc}$ approximation with 6208 number of degrees of freedom for the unknown (\mathbf{u}_h, p_h) with $(\omega=0.1)$. The experimental findings on convergence rates for $\mathbb{P}_1^{nc}/\mathbb{P}_1^{nc}$ FEMs are summarized in Table 3, Table 4 and Figure 6 with $(\omega=1)$ and $(\omega=0.1)$. The desired convergence rates are demonstrated, i.e., the second-order L^2 -errors in velocity and pressure and first-order for H^1 -approximation error in velocity. Moreover, in the $\mathbb{P}_1^{nc}/\mathbb{P}_1^{nc}$ approximations, the stabilized formulation achieves convergence $\mathcal{O}(h^{3/2})$ with respect to GLP norm for the Darcy problem. Furthermore, the numerical simulations are also performed with (3.14) and (4.39) for $\omega=0.01$. As per expectations, the computational results are in agreement with the theoretical predictions.

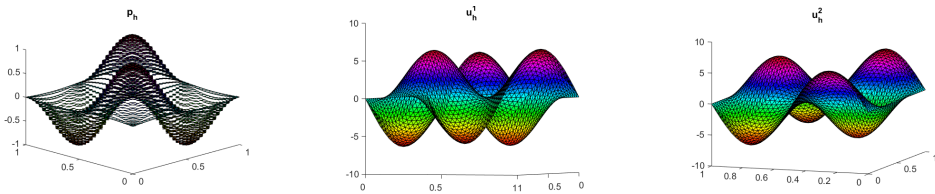


Fig. 3 $\mathbb{P}_1^{nc}/\mathbb{P}_0^{nc}$ GLPS discrete solution (\mathbf{u}_h, p_h) with $(\omega=1, \beta=1)$.

6 Summary

In this article, a generalized local projection stabilized (GLPS) nonconforming finite element scheme for the Darcy equations is two finite element pairs, $(\mathbb{P}_1^{nc}/\mathbb{P}_0)$ and $(\mathbb{P}_1^{nc}/\mathbb{P}_1^{nc})$, was proposed and analyzed. The GLPS technique allows the choice of projection spaces on overlapping sets and avoids using a two-level mesh or enrichment of the finite element space. The partition of unity of the basis functions together with L^2 -orthogonal projection properties is used in deriving the stability and convergence estimates. Further, an *a priori* error analysis is derived for both the finite-dimensional

$\mathbb{P}_1^{nc}/\mathbb{P}_0$ approximations				
Mesh-size h	$\ \mathbf{u}-\mathbf{u}_h\ $	$ \nabla(\mathbf{u}-\mathbf{u}_h) $	$\ p-p_h\ $	$ \cdot _{GLP}$
1/8	1.1803	16.7457	0.3345	0.0071
1/16	0.2953	6.9481	0.1805	0.3490
1/32	0.0803	3.6681	0.0919	0.1223
1/64	0.0232	2.2072	0.0462	0.0517
1/128	0.0071	1.4328	0.0231	0.0242
Order	2	1	1	1

Table 1 Convergence results for $\mathbb{P}_1^{nc}/\mathbb{P}_0$ approximations with $(\omega=1, \beta=1)$.

$\mathbb{P}_1^{nc}/\mathbb{P}_0$ approximations				
Mesh-size h	$\ \mathbf{u}-\mathbf{u}_h\ $	$ \nabla(\mathbf{u}-\mathbf{u}_h) $	$\ p-p_h\ $	$ \cdot _{GLP}$
1/8	1.1178	14.5783	0.3978	3.5660
1/16	0.2822	6.2639	0.1869	0.9129
1/32	0.0709	2.8722	0.0928	0.2430
1/64	0.0178	1.3764	0.0463	0.0730
1/128	0.0044	0.6778	0.0231	0.0271
Order	2	1	1	1

Table 2 Convergence results for $\mathbb{P}_1^{nc}/\mathbb{P}_0$ approximations with $(\omega=0.1, \beta=1)$.

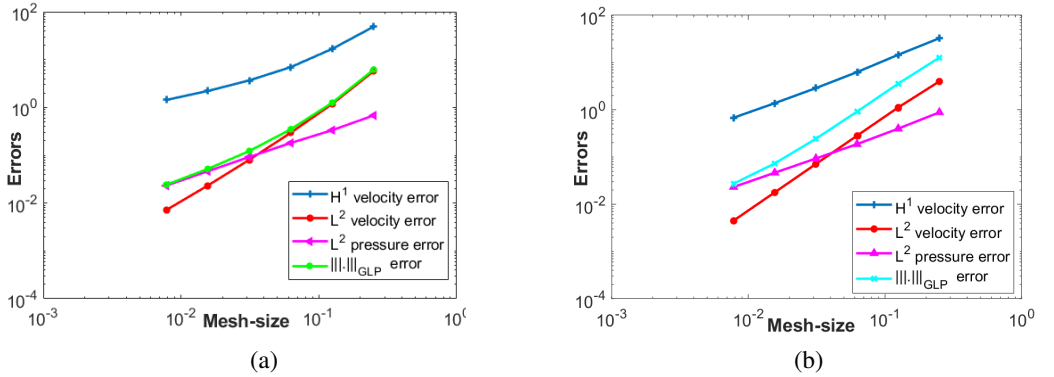


Fig. 4 Convergence plots of $\mathbb{P}_1^{nc}/\mathbb{P}_0$ approximation with (a) $(\omega=1, \beta=1)$ and (b) $(\omega=0.1, \beta=1)$.

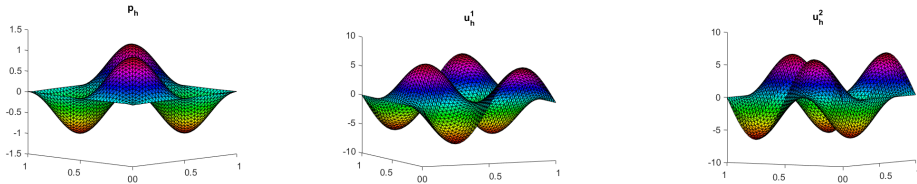


Fig. 5 $\mathbb{P}_1^{nc}/\mathbb{P}_1^{nc}$ GLPS discrete solution (\mathbf{u}_h, p_h) with $(\omega=0.1, \beta=1)$.

$\mathbb{P}_1^{nc}/\mathbb{P}_1^{nc}$ approximations				
Mesh-size h	$\ \mathbf{u}-\mathbf{u}_h\ $	$ \nabla(\mathbf{u}-\mathbf{u}_h) $	$\ p-p_h\ $	$\ \cdot\ _{GLP}$
1/8	1.1575	15.8431	0.2144	1.3909
1/16	0.3012	7.0575	0.0405	0.3741
1/32	0.0809	3.7293	0.0073	0.0861
1/64	0.0233	2.2368	0.0017	0.02451
1/128	0.0071	1.4475	0.0004	0.0075
Order	2	1	2	1.5

Table 3 Convergence results for $\mathbb{P}_1^{nc}/\mathbb{P}_1^{nc}$ approximations with $(\omega=1, \beta=1)$.

$\mathbb{P}_1^{nc}/\mathbb{P}_1^{nc}$ approximations				
Mesh-size h	$\ \mathbf{u}-\mathbf{u}_h\ $	$ \nabla(\mathbf{u}-\mathbf{u}_h) $	$\ p-p_h\ $	$\ \cdot\ _{GLP}$
1/8	1.0034	11.9293	0.2414	10.0536
1/16	0.2678	5.1942	0.0486	2.6825
1/32	0.0691	2.5644	0.0114	0.6920
1/64	0.0176	1.2948	0.0033	0.1762
1/128	0.0044	0.6565	0.0009	0.0446
Order	2	1	2	1.5

Table 4 Convergence results for $\mathbb{P}_1^{nc}/\mathbb{P}_1^{nc}$ approximations with $(\omega=0.1, \beta=1)$.

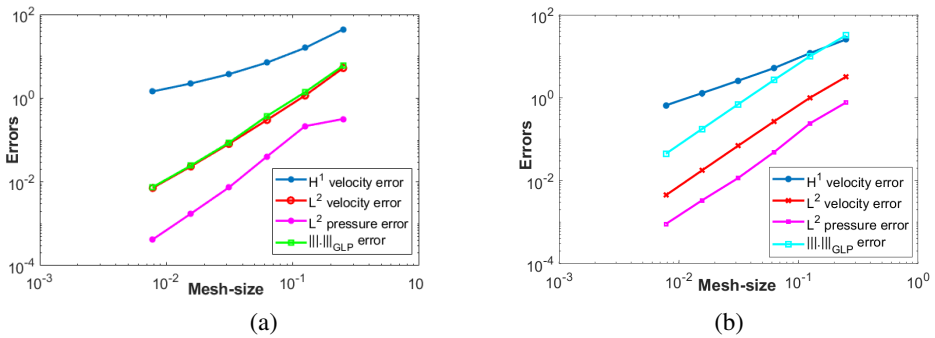


Fig. 6 Convergence plots of $\mathbb{P}_1^{nc}/\mathbb{P}_1^{nc}$ approximations with (a) $(\omega=1, \beta=1)$ and (b) $(\omega=0.1, \beta=1)$.

approximations. An array of numerical experiments is presented to support the derived estimates and demonstrate the proposed scheme's efficiency in suppressing the oscillations without compromising convergence.

Acknowledgments

The first author would like to thank the Tata Trusts traveling grants (ODAA/INT/19/189) and the National Mathematics Initiative (NMI), Department of Mathematics, Indian Institute of Science,

Bengaluru, India. Further, this work is partially supported by the Science and Engineering Research Board (SERB), Department of Science and Technology, Government of India, with the grant EMR/2016/003412.

References

1. Randolph E Bank and Harry Yserentant. On the H^1 -stability of the L_2 -projection onto finite element spaces. *Numer. Math.*, 126(2):361–381, 2014.
2. Roland Becker and Malte Braack. A finite element pressure gradient stabilization for the Stokes equations based on local projections. *Calcolo*, 38(4):173–199, 2001.
3. Luca Bergamaschi, Stefano Mantica, and Gianmarco Manzini. A Mixed Finite Element-Finite Volume Formulation of the Black-Oil Model. *SIAM J. Sci. Comput.*, 20(3):970–997, 1998.
4. Rahul Biswas, Asha K. Dond, and Thirupathi Gudi. Edge patch-wise local projection stabilized nonconforming FEM for the Oseen problem. *Comput. Methods Appl. Math.*, 19(2):189–214, 2019.
5. Pavel B Bochev and Clark R Dohrmann. A computational study of stabilized, low-order C^0 finite element approximations of Darcy equations. *Comput. Mech.*, 38(4-5):323–333, 2006.
6. PB Bochev and MD Gunzburger. A locally conservative least-squares method for Darcy flows. *Comm. Numer. Methods Engrg.*, 24(2):97–110, 2008.
7. M. Braack. Optimal control in fluid mechanics by finite elements with symmetric stabilization. *SIAM J. Control Optim.*, 48(2):672–687, 2009.
8. M Braack and F Schieweck. Equal-order finite elements with local projection stabilization for the Darcy–Brinkman equations. *Comput. Methods Appl. Mech. Engrg.*, 200(9-12):1126–1136, 2011.
9. Malte Braack and Erik Burman. Local projection stabilization for the Oseen problem and its interpretation as a variational multiscale method. *SIAM J. Numer. Anal.*, 43(6):2544–2566, 2006.
10. Susanne C. Brenner and L Ridgway Scott. *The mathematical theory of finite element methods*. Springer-Verlag, New York, 2008.
11. Franco Brezzi, Jim Douglas, Ricardo Durán, and Michel Fortin. Mixed finite elements for second order elliptic problems in three variables. *Numer. Math.*, 51(2):237–250, 1987.
12. Franco Brezzi, Jim Douglas, Jr., and L. D. Marini. Two families of mixed finite elements for second order elliptic problems. *Numer. Math.*, 47(2):217–235, 1985.
13. Franco Brezzi, Michel Fortin, L Donatella Marini, et al. Efficient rectangular mixed finite elements in two and three space variables. *ESAIM Math. Model. Numer. Anal.*, 21(4):581–604, 1987.
14. Erik Burman and Alexandre Ern. A Continuous finite element method with Face penalty to approximate Friedrichs’ systems. *M2AN Math. Model. Numer. Anal.*, 41(1):55–76, 2007.
15. Erik Burman and Peter Hansbo. Stabilized Crouzeix-Raviart element for the Darcy-Stokes problem. *Numer. Methods Partial Differential Equations*, 21(5):986–997, 2005.
16. Erik Burman and Peter Hansbo. A stabilized non-conforming finite element method for incompressible flow. *Comput. Methods Appl. Mech. Engrg.*, 195(23-24):2881–2899, 2006.
17. Erik Burman and Peter Hansbo. A unified stabilized method for Stokes’ and Darcy’s equations. *J. Comput. Appl. Math.*, 198(1):35–51, 2007.
18. G Chavent, G Cohen, and J Jaffre. Discontinuous upwinding and mixed finite elements for two-phase flows in reservoir simulation. *Comput. Methods Appl. Mech. Engrg.*, 47(1-2):93–118, 1984.
19. Zhangxin Chen. *Finite element methods and their applications*. Springer Science & Business Media, 2005.
20. M. Crouzeix and P.-A. Raviart. Conforming and nonconforming finite element methods for solving the stationary Stokes equations. I. *Rev. Française Automat. Informat. Recherche Opérationnelle Sér. Rouge*, 7(R-3):33–75, 1973.
21. Daniele Antonio Di Pietro and Alexandre Ern. *Mathematical aspects of discontinuous Galerkin methods*, volume 69. Springer Science & Business Media, 2011.
22. Asha K Dond and Thirupathi Gudi. Patch-wise local projection stabilized finite element methods for convection–diffusion–reaction problems. *Numer. Methods Partial Differential Equations*, 35(2):638–663, 2019.

23. Jim Douglas, Jr., Felipe Pereira, and Li-Ming Yeh. A locally conservative Eulerian-Lagrangian numerical method and its application to nonlinear transport in porous media. *Comput. Geosci.*, 4(1):1–40, 2000.
24. Louis J Durlafsky. Accuracy of mixed and control volume finite element approximations to Darcy velocity and related quantities. *Water Resources Research*, 30(4):965–973, 1994.
25. A Ern and JL Guermond. Theory and practice of finite elements springer-verlag. *New York*, 2004.
26. RE Ewing and RF Heinemann. Mixed finite element approximation of phase velocities in compositional reservoir simulation. *Comput. Methods Appl. Mech. Engrg*, 47(1-2):161–175, 1984.
27. Richard E Ewing, Thomas F Russell, and Mary Fanett Wheeler. Convergence analysis of an approximation of miscible displacement in porous media by mixed finite elements and a modified method of characteristics. *Comput. Methods Appl. Mech. Engrg.*, 47(1-2):73–92, 1984.
28. Sashikumar Ganesan, Gunar Matthies, and Lutz Tobiska. Local projection stabilization of equal order interpolation applied to the Stokes problem. *Math. Comp.*, 77(264):2039–2060, 2008.
29. Sashikumar Ganesan and Lutz Tobiska. Stabilization by local projection for convection–diffusion and incompressible flow problems. *J. Sci. Comput.*, 43(3):326–342, 2010.
30. D. Garg and S. Ganesan. Generalized local projection stabilized finite element method for Advection-reaction problems. *Communicated*.
31. Jean-Luc Guermond. Subgrid stabilization of Galerkin approximations of linear monotone operators. *IMA J. Numer. Anal.*, 21(1):165–197, 2001.
32. Volker John, Petr Knobloch, and Simona B. Savescu. A posteriori optimization of parameters in stabilized methods for convection-diffusion problems - Part I. *Comput. Methods Appl. Mech. Engrg.*, 200:2916–2929, 2011.
33. Petr Knobloch. A generalization of the local projection stabilization for convection-diffusion-reaction equations. *SIAM J. Numer. Anal.*, 48(2):659–680, 2010.
34. Petr Knobloch and Lutz Tobiska. On the stability of finite-element discretizations of convection-diffusion-reaction equations. *IMA J. Numer. Anal.*, 31(1):147–164, 2011.
35. Petr Knobloch and Lutz Tobiska. Improved stability and error analysis for a class of local projection stabilizations applied to the Oseen problem. *Numer. Methods Partial Differential Equations*, 29(1):206–225, 2013.
36. Kent Andre Mardal, Xue-Cheng Tai, and Ragnar Winther. A robust finite element method for Darcy–Stokes flow. *SIAM J. Numer. Anal.*, 40(5):1605–1631, 2002.
37. Arif Masud and Thomas JR Hughes. A stabilized mixed finite element method for Darcy flow. *Comput. Methods Appl. Mech. Engrg.*, 191(39-40):4341–4370, 2002.
38. Kamel Nafa. Local projection finite element stabilization for Darcy flow. *Int. J. Numer. Anal. Model.*, 7(4):656–666, 2010.
39. Pierre-Arnaud Raviart and Jean-Marie Thomas. A mixed finite element method for 2-nd order elliptic problems. In *Mathematical aspects of finite element methods*, pages 292–315. Springer, 1977.
40. Hans-Görg Roos, Martin Stynes, and Lutz Tobiska. *Robust numerical methods for singularly perturbed differential equations: convection-diffusion-reaction and flow problems*, volume 24. Springer Science & Business Media, 2008.
41. Lutz Tobiska. On the relationship of local projection stabilization to other stabilized methods for one-dimensional advection-diffusion equations. *Comput. Methods Appl. Mech. Engrg.*, 198(5-8):831–837, 2009.
42. J. Venkatesan and S. Ganesan. Finite element computations of viscoelastic two-phase flows using local projection stabilization. *Int. J. Numer. Meth. Fluids*, DOI: 10.1002/fld.4808, 2020.